Title
Non-Nucleotide Hint1-Labile Phosphoramidates for the Interrogation of Pin1 Biology

Author
Schwarz, Daniel Mark Comins

Publication Date
2021

Peer reviewed|Thesis/dissertation

Non-Nucleotide Hint1-Labile Phosphoramidate Prodrugs for the Interrogation of Pin1 Biology

by

Daniel Mark Comins Schwarz

DISSERTATION

Submitted in partial satisfaction of the requirements for degree of

DOCTOR OF PHILOSOPHY

in

Chemistry and Chemical Biology

in the

GRADUATE DIVISION

of the

UNIVERSITY OF CALIFORNIA, SAN FRANCISCO

Approved:

DocuSigned by:
Jason Gestwicki
4909848DBB404E5...

Jason Gestwicki

Chair

DocuSigned by:
LUKE GILBERT
71F73C69F83C48B...

LUKE GILBERT

Kevan Shokat

Committee Members

Dedicated to my loving parents, Raymond Schwarz & Catherine Comins, for their unyielding encouragement for everything I've ever dreamt of doing.

Acknowledgements

Over the past five years, I've learned, grown, and bonded with a group of friends who I have the honor to call "labmates." To me, this title will always be privileged and evoke the simultaneous warmth of love and support with the thrust of intellectual and professional development that has formed the foundation of my time at UCSF. This experience has not only been essential for becoming the scientist I am but has also shaped me into a much better colleague and teammate. Thank you to my labmates, past and present, for everything you've done for me through the years. If you'll forgive the cliché, I couldn't have done this without you, nor would I have wanted to.

To my loving, supportive family: while I could never describe the love and gratitude I have for you in words, I want to take this space to thank you all for every bit of effort that's gone into getting me here. You've been an unwavering source of encouragement as I have navigated through the chapters of my life when I needed it and my all-time favorite people in this world to celebrate. Graduate school has been a constant test of my dedication and my support network. Thank you, Mom, Dad, Kate, Aaron, Jackson, and Hunter for always being there in exactly the right way to keep me moving toward the goals I have in life.

Moving out to the Bay Area has also come with the gift of getting even closer to my amazing cousin, J Zac. You're someone I've always been proud to call family and a best friend. In the past year the pandemic has brought us even closer with countless beach trips, boogies picked, Tuesdays with Tito, and Thicc Thursdays. The greatest thanks to you and the extended family (Tito, Wendy, Kristina, Sharon, and Al) for all the support and love that you've given me. Looking forward to all the Bay Area fun to come!

Non-Nucleotide Hint1-Labile Phosphoramidates for the Interrogation of Pin1 Biology

By Daniel Mark Comins Schwarz

Abstract The peptidyl-prolyl isomerase Pin1 is the only known enzyme capable of isomerizing the peptide bond between pThr/pSer and Pro residues. This bond is extremely rigid and exists in distinct *cis* and *trans* conformations absent the activity of this designated molecular chaperone. Through decades of genetic experiments, Pin1's essentiality in regulating cell cycle progression, apoptosis, and differentiation has been discovered and validated. Interestingly, potent and selective inhibitors of Pin1 were intractable using traditional structure-guided medicinal chemistry as these approaches were capable of yielding only potent *or* biologically active molecules and failed at finding high-affinity molecules which were able to permeate the cell membrane. This is due to the requirement for phosphates for high-affinity reversible binding to the Pin1 catalytic domain. Recently, a handful of efforts using non-traditional approaches to inhibitor design have discovered potent and biologically active molecules. Herein, the design, discovery, validation, and use of the most potent biologically-active Pin1 inhibitor to date is discussed. In this approach, a potent *in vitro* inhibitor of Pin1 discovered by Pfizer is converted to a phosphoramidate-based prodrug to overcome permeability challenges. This approach not only yielded a potent Pin1 inhibitor which could be used in a variety of biological experiments to probe Pin1 biology, but also expanded the understanding of this prodrugging approach. Specifically, the aryloxy phosphoramidate approach has only been described in mechanistic detail with nucleotide phosphoramidates. These proof-of-concept molecules not only show that highly ligand efficient molecules are amenable to this approach but demonstrates that they are liberated through the canonical enzymatic processing. Further, since the parent molecule used is one in a large series of analogs, there is significant SAR around the scaffold which will be useful in future optimization.

Table of Contents

List of Figures

CHAPTER 1

HISTORICAL CHALLENGES IN BIOLOGICAL INHIBITION OF PIN1

Daniel MC Schwarz, Jason E Gestwicki

Background on Chemical Probes. A powerful feature of chemical tools is the speed at which they inhibit function of their target. Unlike genetic approaches that often have long onset times, chemical inhibitors are designed to for a given target can suppress the activity of a target on shorter timescales (1). This feature is especially useful when the target of interest is involved in highly dynamic biology. For example, kinases and epigenetic modifiers act on their substrates on timescales of seconds and minutes (2–4), so chemical probes are perfectly suited to studying their action.

Molecular chaperones are a rich source of targets for chemical probes, due to their rapid and dynamic actions in protein folding. Indeed, natural products and synthetic probes for heat shock protein 70 (Hsp70) and Hsp90 have transformed our understanding of the central roles of these chaperones (5–8). Similarly, the peptidyl-prolyl isomerases (PPIases) are another class of molecular chaperone that are good targets for chemical probes. Briefly, PPIases are responsible for catalyzing the cis/trans isomerization of the omega bond preceding a proline residue (Figure 1.1A) (9–12). These bonds are quite rigid and their isomerization can be rate limiting for protein folding and dynamic (Figure 1.1B) (13). Consequently, PPIase activity regulates protein folding, function and turnover. In part, these discoveries have been enabled through the use of chemical probes. Cyclosporine and FK506 are natural products that bind and inhibit two of the major families of PPIases, the cyclophilins and FK506-binding proteins (FKBPs), respectively. Unfortunately, the third class of PPIases, the parvulins, lacks a *specific* natural product inhibitor (Reviewed in 14).

Among the parvulins, peptidyl-prolyl isomerase NIMA interacting protein 1 (Pin1) has attracted the most effort to design potent and biologically active inhibitors due to its putative role in cancer development and survival.

Despite this substantial effort at inhibiting Pin1, no potent and cell-permeant inhibitor has been discovered (19). This goal is necessary because genetic studies have shown that Pin1 is important in cancer transformation (15–18),

Among the PPIases, Pin1 is unique because it binds and isomerizes proline-directed phosphorylations (pSer/pThr-Pro). To accommodate this charged substrate, Pin1 coordinates the phosphate in a cationic groove comprised of two Arg and one Lys and isomerizes the peptidyl-prolyl bond in a highly solvated catalytic site (Figure 1.2) (20). Additionally, Pin1 can also bind proline-directed phosphorylations non-catalytically with an N-terminal WW domain (21,22).

The structure and charge of the Pin1 active site creates an interesting potency vs. permeability tradeoff; where potent molecules require a strong anion to occupy the cationic groove but this feature reduces cell penetration (23). Recently, there have been a number of innovative solutions to address this foundational challenge (24–26). Here, we survey the progress toward chemical probes for Pin1. We focus special attention on how various groups have approached the problem of balancing physical properties to achieve both selectivity, potency and permeability. We also discuss some of the initial applications of such molecules and how they are revealing new insights into Pin1 biology.

Historical Challenges. The catalytic domain of Pin1 poses challenges to inhibitor discovery and optimization. The cationic groove, which imparts much of the binding energy and specificity of substrate recognition, compliments the di-anionic charge and tetrahedral geometry of a phosphate (Figure 1.2C) (27,28). This complementarity allows for the high degree of selectivity for proline-directed phosphorylation motifs; however, it all but

precludes binding of neutrally charged molecules and even strongly disfavors binding of non-phosphate anions. Additionally, the Pin1 active site is also unusually shallow and solvated, features seen in other protein-protein interactions (PPI) that make them difficult to inhibit (29).

The preference of Pin1 for phosphate-bearing substrates was first outlined in peptide-based experiments and was later supported by lessons learned from small molecule optimization campaigns (20,27). For example, two discovery campaigns ended in failed high throughput screens against Pin1 (30–34), likely because anionic pharmacophores are typically removed from screening libraries due to their synthetic challenges and difficulty in downstream optimization.

Where screening has been unsuccessful, structure-guided drug design has proven more tractable. For instance, Guo et al. started with a known peptide that binds Pin1 (**1**) to create a ligand efficient, phosphate-bearing series of analogs (based off of **2**) (Figure 1.3). These molecules, however, were challenging to optimize into biologically active and potent leads due to the impermeability of the anionic groups. Indeed, the most optimized molecules which were disclosed in the series of publications (the most potent analog shown as **3**) had suffered a 100-fold deterioration in affinity and still had biological EC_{50} values in the low μM range (32–34). Thus, even though structure-based design fared better than HTS, there were still challenges with the balance of charge and permeability.

This limitation of structure-guided, multi-parametric medicinal chemistry has led the Pin1 field in a variety of non-traditional inhibitor development and optimization disciplines. Interestingly, these efforts have been maturing over the past two decades and culminated in multiple, biologically-active Pin1 inhibitors being discovered recently. Interestingly,

multiple, distinct approaches have been employed to solve this core problem. These approaches, their strengths, and their weaknesses will be discussed in the following sections.

Macrocyclic Peptides. Macrocycles and especially macrocyclic peptides have been shown to have far greater membrane permeability than would be expected from their crude physicochemical properties alone. Indeed, the flexibility of the macrocycle allows for differentially lipophilic conformations of the ring where polar groups are exposed to solvent or collapsed within the ring satisfied by intramolecular hydrogen bonding (35–37). Additionally, cyclic peptides (and peptide-based inhibitors in general) can be functionalized with cell penetrating motifs which allow for active transport into the cell by endocytosis (Reviewed in 38). The actively transported peptides are typically less sensitive to anions or other groups which typically preclude passive permeability. Finally, cyclic peptides are excellent inhibitors of protein-protein interactions (PPI), such as the ones between Pin1 and its clients (39), making Pin1 a prime target for this approach.

The crystal structure of Pin1 bound to **1** reveals a beta-turn conformation of the bound peptide (27). Liu and colleagues first used this observation to develop cyclic peptide inhibitors for Pin1 (40). The initial discovery of Pin1-targeting cyclic peptides used a library of unnatural amino acid-containing phosphorylated cyclic peptides (Figure 1.4). These cyclic peptides were screened for competitive binding of the catalytic domain of Pin1 and potent binders were validated by isothermal titration calorimetry (ITC). This screen resulted in low nanomolar binders of which the most potent (**4**) capable of inhibiting Pin1 catalytic activity *in vitro* but lacked cellular activity. While this molecule was putatively active against Pin1 in *in vitro* cell culture, next-generation molecules were produced to incorporate aspects of the commonly-used cell penetrating peptide RKKRRQRRR (aka

HIV Tat peptide (41,42)) into the ring. The most active molecule, **5**, has a permeability advantage; however, the bulky substitutions which do not contribute to binding hindered affinity with an approximate order of magnitude shift in affinity from their non-cell-penetrant analogues.

To overcome the challenge of this permeability potency trade-off, bicyclic peptides were designed which relocated the cell penetrating motif to a second fused macrocycle which does not interact with the target protein (**6**) (43). The most optimized molecule in this campaign retained cellular activity and a 72 nM K_D (less than two-fold worse than the initial molecule which was only optimized for affinity). This series of molecules was able to leverage cell-penetrating peptide sequences as well as retain all of the interaction surface which can be achieved by a macrocycle to block Pin1-client PPIs.

While this approach was able to achieve a potent and cell active Pin1 inhibitor, a few drawbacks are present with this approach. Most immediately, the synthetic feasibility of these molecules is limited. Even for the few labs capable of producing bimacrocyclic peptides, these ones are costly and challenging to synthesize and isolate. This limits access to their use as tool molecules. Further, there is no evidence that these molecules can be used in more complex biological systems. While cell-penetrating peptides has been used in organisms, the pharmacodynamic and pharmacokinetic attributes of these molecules have yet to be demonstrated. Finally, there is limited information available on the nature of the interaction between these molecules and Pin1. Specifically, the binding mode and stoichiometry of binding are unclear. While some of these molecules were evaluated by ITC, the construct of Pin1 used is incapable of binding with its WW domain, which in a WT Pin1 construct would bind proline-directed phosphorylations tightly. While the ability of this molecule to bind both domains would set it apart mechanistically from

others discussed herein, without those data it is challenging to evaluate what binding mode dominates its effects in cells.

Covalent Inhibitors. Covalent inhibitors have a longer history in the Pin1 inhibitor discovery field. Indeed, the first molecule which was classified as a Pin1 inhibitor is a putative covalent modifier of the Cys113 residue in the Pin1 catalytic domain (44). This molecule, Juglone (**6**) is a natural product alkylator (Figure 1.5A) which does elicit a Pin1-dependent toxicity in some contexts. While these data are compelling that **6** operates through at least a partially Pin1-dependent mechanism, this molecule is far from specific (45) and not much is known about its physical interaction with Pin1 in cells. Importantly though, the observed activity of **6** and various structural and enzymological studies drew attention to the highly reactive cysteine in the Pin1 catalytic domain. This Cys113 residues is pK_a-perturbed by a His-His-Cys hydrogen bonding triad similar to those seen in cysteine proteases (46–49). At around a pK_a of 4.0, Cys113 is constitutively deprotonated in physiological pH (48) making it an excellent target for covalent modification.

One of the earlier efforts to rationally design specific covalent modifiers of Pin1 started with a non-covalent carboxylate-containing lead from a medicinal chemistry campaign conducted at Vernalis (**7**) (Figure 1.5B) (30,31). Investigators took this molecule and engineered a Michael acceptor acrylamide into the scaffold aiming to retain the non-covalent affinity from the original molecule while imparting irreversibility to improve the potency (50,51). Interestingly, the most potent molecule in this series (**8**) had an improved K_i over **7** and a promising K_i/k_{inact} of 0.249 $M^{-1} \bullet sec^{-1}$.

Consistent with these measurements, **8** was able to efficiently label Pin1 at Cys113 *in vitro* as confirmed by tryptic peptide LC-MS/MS; however, only modest cellular activity was

observed and conflicting target validation data suggests some non-specific toxicity dominates the anti-proliferative effect. Further, only a mild improvement over the activity of **7**.

Quite recently, further efforts were put into the development of more potent and specific covalent Pin1 inhibitors. One of these efforts began with structural studies of **1** which informed the design of a series of neutrally charged covalent analogs (Figure 1.5C) (24). Briefly, these analogs installed an electrophile proximal to Cys113 in the crystal structure of **1** bound to Pin1 and removed the phosphate which occupies the cationic groove. The hypothesis was while neutral analogs would allow for cell permeability, the covalent binding to the Pin1 catalytic domain would drive affinity and the remaining optimized ligand would drive specificity. Each analog was subject to a fluorescence polarization competition binding assay in which a fluorescent analog of **1** was competed off of the isolated Pin1 catalytic domain. Binders were subsequently tested for inhibitory activity in the fluorogenic Pin1 PPIase activity assay, labeling confirmation by whole-protein MS, and binding mode elucidation by x-ray crystallography.

The lead molecule from this campaign, **9**, was demonstrated to inhibit Pin1 *in vitro* with an IC_{50} of 48 nM after 12 hours and confirmed as a single labeling event of Pin1 by whole-protein MS. Impressively, when subject to an unbiased dose-responsive labeling proteomics experiment called CITe-Id (52) , Pin1 Cys113 is by far the most dose-responsively labeled peptide in the proteome supporting **9** as an exceptionally selective Pin1 inhibitor. Another value of this effort was the discovery of the control molecule **10** which lacks the electrophile and subsequent ability to bind and inhibit Pin1 catalytic domain (IC_{50} >> 100 μM).

Further studies with **9** further validate that various biological effects may be attributed to Pin1-specific activity including antiproliferative activity against some c-Myc-dependent cell lines and cooperativity with $KRAS^{G12V}$ degradation. While the cellular activity of **9** is satisfactory and the covalent specificity is exceptional, no *in vivo* activity has been demonstrated.

Concurrent with the development of **9**, an effort to discover a lower molecular weight covalent inhibitor of Pin1 was conducted by an overlapping group of investigators (Figure 1.5D) (25). This effort began with a covalent fragment screening campaign in which 933 electrophilic fragments were tested for labeling of the Pin1 active cite Cys113. From this screen, a plurality of hits contained a cyclic sulfone – a unique enrichment as compared to previous screens with this library against distinct proteins.

The investigators consequently promoted the most potent fragment with this structural feature (**11**) as a core scaffold and synthesized a small library of analogs. This library of 26 molecules produced 25 molecules which modified Pin1 more potently than **11** in a MS-based labeling. Of these molecules, one lacked non-specific toxicity when tested in lung fibroblasts. This molecule, **12**, was promoted as the lead molecule and tested further. Among the methods of evaluation of target engagement, cells were treated with the desthiobiotinylated analog of **12**, **13**. This tool molecule was able to pull down Pin1 competitively with **12** in a competition affinity purification experiment in cells supporting a potent binding event. Importantly, this experiment could be repeated in mice where **12** was dosed by oral gavage and spleen lysate was affinity purified with **13**. A dose-responsive competition was observed. Notably, the *in vivo* experiments conducted with **12** shed little light on the bioavailability and distribution of the molecule as all were assessing the activity of **12** on blood cells or in the spleen which is a highly vascularized organ.

Finally, to assess the specificity of **12**, cells were subject to the aforementioned CITe-Id approach in which Pin1 Cys113 was again enriched as a unique specifically modified peptide.

These results suggest a very promising starting point for developing a potent and selective covalent Pin1 inhibitor. Covalent approaches have clearly circumvented some of the challenges with getting potent Pin1 inhibitors into cells and to some degree complex organisms. While this is certainly an achievement, these were substantial efforts to optimize specificity, potency, and bioavailability which ultimately produced modestly active molecules with biological distribution only demonstrated in the blood of the most bioavailable molecule.

Phosphate Prodrugs. Numerous peptide and small molecule biochemical and structural experiments have confirmed the preferential binding of Pin1 to phosphates over various bioisosteres. For instance, in the seminal paper defining the sequence specificity of Pin1 identified pSer and pThr preference over even Glu by a respective 2- or 3-order difference in catalytic efficiency (20). In the context of small molecule inhibition, in two extensive medicinal chemistry campaigns by Pfizer and Vernalis, Pin1 inhibitors with direct substitution of a phosphate with traditional bioisosteres suffered similar potency losses (Reviewed in 19).

A common approach for overcoming this is to use metabolically and/or chemically labile prodrugs (53). These molecules are typically neutral in charge and are capable of undergoing some chemical transformation under physiological conditions to liberate the parent molecule with an intact phosphate or phosphonate.

The first phosphate prodrug for the inhibition of Pin1 was designed from an alkene cis peptidyl-prolyl isostere peptide inhibitor **14** (Figure 1.6) (54). The in vitro IC_{50} (1.3 μM) and binding mode of **14** had been previously characterized in other biochemical and structural work; however, the biological effects of this substrate-competitive binding were elusive due to the weak biological activity (A2780 GI_{50} 46.2 μM) likely due to membrane permeability. The caging of the phosphate with a bis-pivaloyloxymethyl (bis-POM) caging group afforded the membrane permeant prodrug **15** (55). This improvement on membrane permeability led to a 2-fold gain in cellular potency over the parent phosphate (A2780 GI_{50} 26.9 μM).

Unfortunately, further biological characterization of this molecule has not been published. One can imagine a few challenges driving this. The parent molecule **14**, while an effective *in vitro* inhibitor of Pin1, has modest affinity for the protein and therefore would potentially bind other targets in the cell at an effective dose. Additionally, Bis-POM prodrugs are quite useful for cell-based experiments; however, their instability in serum and rapid liberation kinetics make them poorly bioavailable (56). At the time of discovery of **15**, these limitations likely made other approaches to the biological inhibition of Pin1 favorable.

Recently, though, major advances and human proof-of-concept have been achieved in the nucleotide field to develop highly controllable and serum-stable phosphoramidate prodrugs (so-called ProTides) (57–60). Additionally, since the discovery of **15**, highly ligand efficient phosphorylated inhibitors of Pin1 have been published by Pfizer and Vernalis during extensive structure-guided and fragment evolution medicinal chemistry campaigns, respectively (30–34). Given the preponderance of recent advances, the following work has been focused on validating the phosphoramidate approach for use in

non-nucleotide phosphate prodrugs to be used as potent inhibitors of Pin1 in in-tact biological systems.

References

1. Arrowsmith CH, Audia JE, Austin C, Baell J, Bennett J, Blagg J, et al. The promise and peril of chemical probes. Nat Chem Biol. 2015;11(8):536–41.
2. Zhao Q, Ouyang X, Wan X, Gajiwala KS, Kath JC, Jones LH, et al. Broad-spectrum kinase profiling in live cells with lysine-targeted sulfonyl fluoride probes. J Am Chem Soc. 2017;139(2):680–5.
3. Horning BD, Suciu RM, Ghadiri DA, Ulanovskaya OA, Matthews ML, Lum KM, et al. Chemical Proteomic Profiling of Human Methyltransferases. J Am Chem Soc. 2016;138(40):13335–43.
4. Arrowsmith CH, Bountra C, Fish P V, Lee K, Schapira M. Epigenetic protein families: a new frontier for drug discovery. Nat Rev Drug Discov [Internet]. 2012;11(5):384–400. Available from: http://dx.doi.org/10.1038/nrd3674%5Cnhttp://www.ncbi.nlm.nih.gov/pubmed/22498752
5. Freilich R, Arhar T, Abrams JL, Gestwicki JE. Protein-Protein Interactions in the Molecular Chaperone Network. Acc Chem Res. 2018;51(4):940–9.
6. Neckers L, Workman P. Hsp90 molecular chaperone inhibitors: Are we there yet? Clin Cancer Res. 2012;18(1):64–76.
7. Gestwicki JE, Shao H. Inhibitors and chemical probes for molecular chaperone networks. J Biol Chem [Internet]. 2019;294(6):2151–61. Available from: http://dx.doi.org/10.1074/jbc.TM118.002813
8. Zhong M, Lee GM, Sijbesma E, Ottmann C, Arkin MR. Modulating protein–protein interaction networks in protein homeostasis. Curr Opin Chem Biol [Internet]. 2019;50:55–65. Available from: https://doi.org/10.1016/j.cbpa.2019.02.012
9. Schiene-Fischer C. Multidomain Peptidyl Prolyl cis/trans Isomerases. Biochim Biophys Acta - Gen Subj [Internet]. 2015;1850(10):2005–16. Available from: http://dx.doi.org/10.1016/j.bbagen.2014.11.012

10. Davis TL, Walker JR, Campagna-Slater V, Finerty PJ, Finerty PJ, Paramanathan R, et al. Structural and biochemical characterization of the human cyclophilin family of peptidyl-prolyl isomerases. PLoS Biol. 2010;8(7).
11. Kumari S, Roy S, Singh P, Singla-Pareek SL, Pareek A. Cyclophilins: Proteins in search of function. Plant Signal Behav. 2013;8(1):25–32.
12. Tong M, Jiang Y. FK506-Binding Proteins and Their Diverse Functions. Curr Mol Pharmacol. 2015;9(1):48–65.
13. Craveur P, Joseph AP, Poulain P, De Brevern AG, Rebehmed J. Cis-trans isomerization of omega dihedrals in proteins. Amino Acids. 2013;45(2):279–89.
14. Dunyak BM, Gestwicki JE. Peptidyl-Proline Isomerases (PPIases): Targets for Natural Products and Natural Product-Inspired Compounds. J Med Chem [Internet]. 2016;acs.jmedchem.6b00411. Available from: http://pubs.acs.org/doi/abs/10.1021/acs.jmedchem.6b00411
15. Gianni' M, Boldetti A, Guarnaccia V, Rambaldi A, Parrella E, Raska I, et al. Inhibition of the peptidyl-prolyl-isomerase Pin1 enhances the responses of acute myeloid leukemia cells to retinoic acid via stabilization of RARα and PML-RARα. Cancer Res. 2009;69(3):1016–26.
16. Min S, Min S, Min S, Ping K, Lu L, Lee A. Archives of Pharmacal Research The role of Pin1 in the development and treatment of cancer. Arch Pharm Res. 2013;
17. Lu Z, Hunter T. Prolyl isomerase Pin1 in cancer. Cell Res [Internet]. 2014;24(9):1033–49. Available from: http://www.pubmedcentral.nih.gov/articlerender.fcgi?artid=4152735&tool=pmcentrez&rendertype=abstract
18. Ryo A, Uemura H, Ishiguro H, Saitoh T, Yamaguchi A, Perrem K, et al. Stable suppression of tumorigenicity by Pin1-targeted RNA interference in prostate cancer. Clin Cancer Res. 2005;11(20):7523–31.

19. Moore JD, Potter A. Pin1 inhibitors: Pitfalls, progress and cellular pharmacology. Bioorganic Med Chem Lett [Internet]. 2013;23(15):4283–91. Available from: http://dx.doi.org/10.1016/j.bmcl.2013.05.088

20. Yaffe MB, Schutkowski M, Shen M, Zhou XZ, Stukenberg PT, Rahfeld JU, et al. Sequence-specific and phosphorylation dependent proline isomerization: A potential mitotic regulatory mechanism. Science (80-). 1997;278(5345):1957–60.

21. Verdecia MA, Bowman ME, Lu KP, Hunter T, Noel JP. Structural basis for phosphoserine-proline recognition by group IV WW domains. Nat Struct Biol. 2000;7(8):639–43.

22. Lu P. Function of WW Domains as Phosphoserine- or Phosphothreonine-Binding Modules. Science (80-) [Internet]. 1999;283(5406):1325–8. Available from: http://www.sciencemag.org/cgi/doi/10.1126/science.283.5406.1325

23. Lelkes PI, Bach D, Miller IR. Perturbations of Membrane Structure by Optical Probes: II. Differential Scanning Calorimetry of Dipalmitoyllecithin and Its Analogs Interacting with Merocyanine 540. J Membr Biol. 1980;54:141–8.

24. Pinch BJ, Doctor ZM, Nabet B, Browne CM, Seo HS, Mohardt ML, et al. Identification of a potent and selective covalent Pin1 inhibitor. Nat Chem Biol [Internet]. 2020; Available from: http://dx.doi.org/10.1038/s41589-020-0550-9

25. Dubiella C, Pinch BJ, Koikawa K, Zaidman D, Poon E, Manz TD, et al. Sulfopin is a covalent inhibitor of Pin1 that blocks Myc-driven tumors in vivo. Nat Chem Biol [Internet]. 2021; Available from: http://www.ncbi.nlm.nih.gov/pubmed/33972797

26. Schwarz DMC, Williams SK, Dillenburg M, Wagner CR, Gestwicki JE. A Phosphoramidate Strategy Enables Membrane Permeability of a Non-nucleotide Inhibitor of the Prolyl Isomerase Pin1. ACS Med Chem Lett. 2020;11(9):1704–10.

27. Zhang Y, Daum S, Wildermann D, Zhou XZ, Verdecia MA, Bowman ME, et al. Structural basis for high-affinity peptide inhibition of human Pin1. ACS Chem Biol. 2007;2(5):320–8.

28. Hirsch AKH, Fischer FR, Diederich F. Phosphate recognition in structural biology. Angew Chemie - Int Ed. 2007;46(3):338–52.

29. Arkin MR, Tang Y, Wells JA. Review Small-Molecule Inhibitors of Protein-Protein Interactions : Progressing toward the Reality. Chem Biol [Internet]. 2014;21(9):1102–14. Available from: http://dx.doi.org/10.1016/j.chembiol.2014.09.001

30. Potter AJ, Ray S, Gueritz L, Nunns CL, Bryant CJ, Scrace SF, et al. Structure-guided design of α-amino acid-derived Pin1 inhibitors. Bioorganic Med Chem Lett [Internet]. 2010;20(2):586–90. Available from: http://dx.doi.org/10.1016/j.bmcl.2009.11.090

31. Potter A, Oldfield V, Nunns C, Fromont C, Ray S, Northfield CJ, et al. Discovery of cell-active phenyl-imidazole Pin1 inhibitors by structure-guided fragment evolution. Bioorganic Med Chem Lett [Internet]. 2010;20(22):6483–8. Available from: http://dx.doi.org/10.1016/j.bmcl.2010.09.063

32. Guo C, Hou X, Dong L, Dagostino E, Greasley S, Ferre R, et al. Structure-based design of novel human Pin1 inhibitors (I). Bioorganic Med Chem Lett [Internet]. 2009;19:5613–6. Available from: http://dx.doi.org/10.1016/j.bmcl.2009.08.034

33. Dong L, Marakovits J, Hou X, Guo C, Greasley S, Dagostino E, et al. Structure-based design of novel human Pin1 inhibitors (II). Bioorganic Med Chem Lett. 2010;20:2210–4.

34. Guo C, Hou X, Dong L, Marakovits J, Greasley S, Dagostino E, et al. Structure-based design of novel human Pin1 inhibitors (III): Optimizing affinity beyond the phosphate recognition pocket. Bioorganic Med Chem Lett [Internet]. 2014;24(17):4187–91. Available from: http://dx.doi.org/10.1016/j.bmcl.2014.07.044

35. Rezai T, Yu B, Millhauser GL, Jacobson MP, Lokey RS. Testing the conformational hypothesis of passive membrane permeability using synthetic cyclic peptide diastereomers. J Am Chem Soc. 2006;128(8):2510–1.

36. Qin Wang, Simone Sciabola, Gabriela Barreiro, Xinjun Hou, Guoyun Bai, Michael J. Shapiro, Frank Koehn, Anabella Villalobos and MPJ. Dihedral Angle-Based Sampling of

Natural Product Polyketide Conformations: Application to Permeability Prediction.

37. Cortez FDJ, Nguyen P, Truillet C, Tian B, Kuchenbecker KM, Evans MJ, et al. Development of 5N-Bicalutamide, a High-A ffi nity Reversible Covalent Antiandrogen. 2017;

38. Guidotti G, Brambilla L, Rossi D. Cell-Penetrating Peptides: From Basic Research to Clinics. Trends Pharmacol Sci [Internet]. 2017;38(4):406–24. Available from: http://dx.doi.org/10.1016/j.tips.2017.01.003

39. Qvit N, Rubin SJS. Cyclic Peptides for Protein-Protein Interaction Targets. Curr Top Med Chem. 2018;18(7):525–525.

40. Liu T, Liu Y, Kao H-Y, Pei D. Membrane Permeable Cyclic Peptidyl Inhibitors against Human Peptidylprolyl Isomerase Pin1. J Med Chem [Internet]. 2010 Mar 25 [cited 2017 Mar 12];53(6):2494–501. Available from: http://pubs.acs.org/doi/abs/10.1021/jm901778v

41. Vivès E, Brodin P, Lebleu B. A truncated HIV-1 Tat protein basic domain rapidly translocates through the plasma membrane and accumulates in the cell nucleus. J Biol Chem. 1997;272(25):16010–7.

42. Elliott G, O'Hare P. Intercellular trafficking and protein delivery by a herpesvirus structural protein. Cell. 1997;88(2):223–33.

43. Lian W, Jiang B, Qian Z, Pei D. Cell-permeable bicyclic peptide inhibitors against intracellular proteins. J Am Chem Soc. 2014;136(28):9830–3.

44. Hennig L, Christner C, Kipping M, Schelbert B, Rücknagel KP, Grabley S, et al. Selective inactivation of parvulin-like peptidyl-prolyl cis/trans isomerases by juglone. Biochemistry. 1998;37(17):5953–60.

45. Fila C, Metz C, Van Der Sluijs P. Juglone inactivates cysteine-rich proteins required for progression through mitosis. J Biol Chem [Internet]. 2008;283(31):21714–24. Available from: http://dx.doi.org/10.1074/jbc.M710264200

46. Wang J, Kawasaki R, Uewaki J ichi, Rashid AUR, Tochio N, Tate S ichi. Dynamic

allostery modulates catalytic activity by modifying the hydrogen bonding network in the catalytic site of human Pin1. Molecules. 2017;22(6).

47. Xu N, Tochio N, Wang J, Tamari Y, Uewaki JI, Utsunomiya-Tate N, et al. The C113D mutation in human Pin1 causes allosteric structural changes in the phosphate binding pocket of the ppiase domain through the tug of war in the dual-histidine motif. Biochemistry. 2014;53(34):5568–78.

48. Behrsin CD, Bailey ML, Bateman KS, Hamilton KS, Wahl LM, Brandl CJ, et al. Functionally Important Residues in the Peptidyl-prolyl Isomerase Pin1 Revealed by Unigenic Evolution. J Mol Biol. 2007;365(4):1143–62.

49. Ikura T, Yonezawa Y, Ito N. Mutational effects of Cys113 on structural dynamics of Pin1. Biophys Physicobiology. 2019;16(0):452–65.

50. Nakagawa H, Seike S, Sugimoto M, Ieda N, Kawaguchi M, Suzuki T, et al. Peptidyl prolyl isomerase Pin1-inhibitory activity of d-glutamic and d-aspartic acid derivatives bearing a cyclic aliphatic amine moiety. Bioorganic Med Chem Lett [Internet]. 2015;25(23):5619–24. Available from: http://dx.doi.org/10.1016/j.bmcl.2015.10.033

51. Ieda N, Itoh K, Inoue Y, Izumiya Y, Kawaguchi M, Miyata N, et al. An irreversible inhibitor of peptidyl-prolyl cis/trans isomerase Pin1 and evaluation of cytotoxicity. Bioorganic Med Chem Lett. 2019 Feb 1;29(3):353–6.

52. Browne CM, Jiang B, Ficarro SB, Doctor ZM, Johnson JL, Card JD, et al. A Chemoproteomic Strategy for Direct and Proteome-Wide Covalent Inhibitor Target-Site Identification. J Am Chem Soc. 2019;141(1):191–203.

53. Wiemer AJ, Wiemer DF. Prodrugs of phosphonates and phosphates: crossing the membrane barrier. Top Curr Chem. 2015;360:115–60.

54. Wang XJ, Xu B, Mullins AB, Neiler FK, Etzkorn FA. Conformationally locked isostere of phosphoSer-cis-Pro inhibits Pin1 23-fold better than phosphoSer-trans-Pro isostere. J Am Chem Soc. 2004;126(47):15533–42.

55. Zhao S, Etzkorn FA. A phosphorylated prodrug for the inhibition of Pin1. Bioorganic Med Chem Lett. 2007;17(23):6615–8.

56. Benzaria S, Pélicano H, Johnson R, Maury G, Imbach JL, Aubertin AM, et al. Synthesis, in vitro antiviral evaluation, and stability studies of bis(s-acyl-2-thioethyl) ester derivatives of 9-[2- (phosphonomethoxy)ethyl]adenine (PMEA) as potential PMEA prodrugs with improved oral bioavailability. J Med Chem. 1996;39(25):4958–65.

57. McGuigan C, Devine KG, O'Connor TJ, Kinchington D. Synthesis and anti-HIV activity of some haloalkyl phosphoramidate derivatives of 3′-azido-3′-deoxythymidine (AZT): potent activity of the trichloroethyl methoxyalaninyl compound. Antiviral Res. 1991;15(3):255–63.

58. Curley D, McGuigan C, Devine KG, O'Connor TJ, Jeffries DJ, Kinchington D. Synthesis and anti-HIV evaluation of some phosphoramidate derivatives of AZT: Studies on the effect of chain elongation on biological activity. Antiviral Res. 1990;14(6):345–56.

59. Slusarczyk M, Serpi M, Pertusati F. Phosphoramidates and phosphonamidates (ProTides) with antiviral activity. Vol. 26, Antiviral Chemistry and Chemotherapy. 2018. 1–31 p.

60. Mehellou Y, Rattan HS, Balzarini J. The ProTide Prodrug Technology: From the Concept to the Clinic. J Med Chem. 2018;61(6):2211–26.

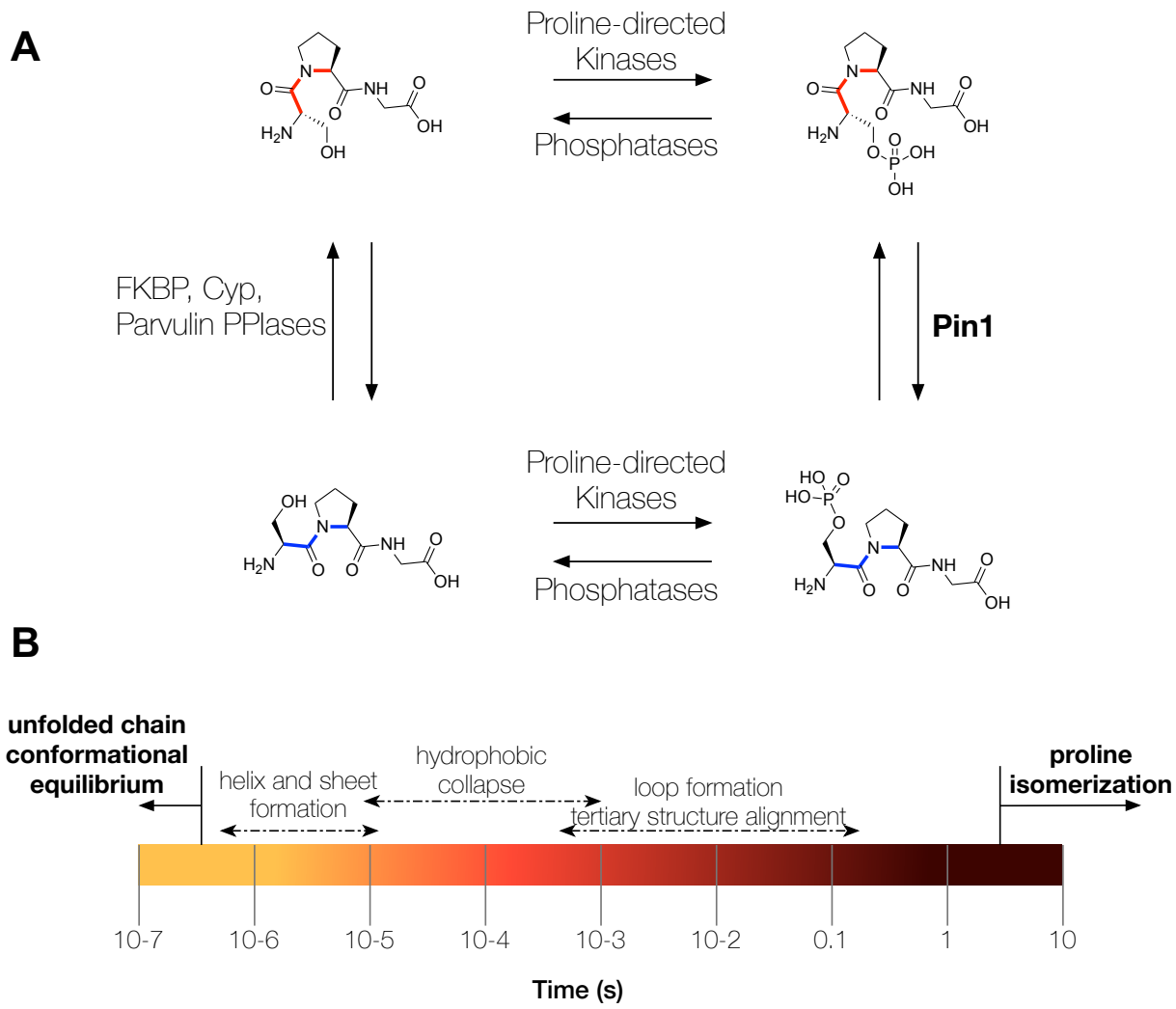

Figure 1.1. Peptidyl-prolyl bond isomerization in the context of proline-directed phosphorylation. A) Proline-directed phosphorylations exist in a four-part equilibrium. The first axis based on phosphorylation and dephosphorylation, which is dependent on conformationally biased, proline-directed kinases and phosphatases. Then, PPIases enable rapid conformational transitions through proline isomerization. While various PPIases are capable for isomerizing unphosphorylated Ser/Thr-Pro bonds, Pin1 is the only known PPIase to isomerize pSer/pThr-Pro bonds. B) Peptidyl-prolyl bonds isomerize on a timescale which is relatively slow and can be rate-limiting. Indeed, the rate of isomerization of prolines was first discovered while studying the kinetics of protein folding and was found to be rate limiting for *in vitro* protein folding in the absence of molecular chaperones.

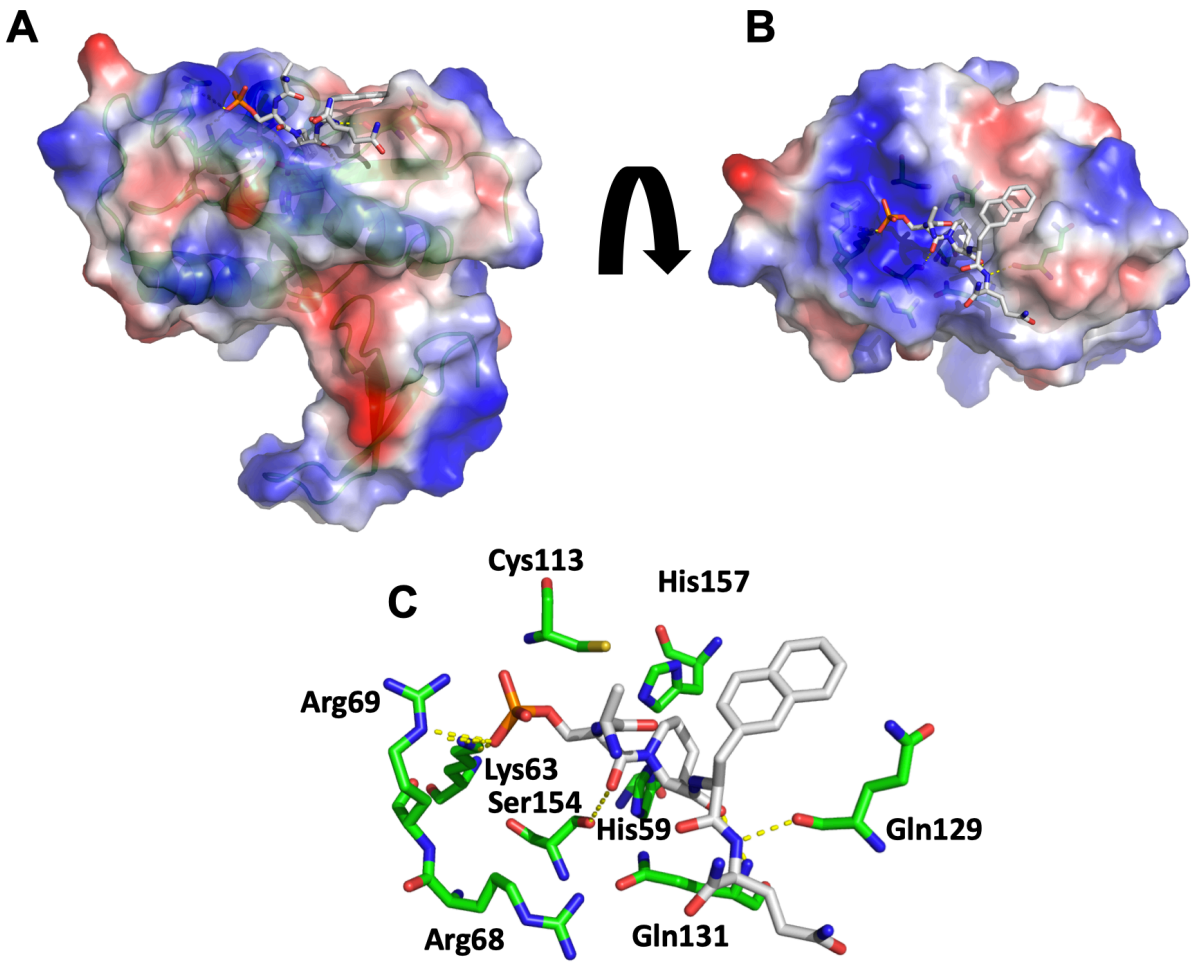

Figure 1.2. Co-crystal structure of Pin1 with Pintide (1) outlines key interactions required for high-affinity binding to the Pin1 catalytic domain. A) Side view of R14A mutant Pin1 bound to the unnatural amino acid peptide "Pintide" (also referred to as **1**, see Figure 1.3). Pintide binds both to catalytic (as seen) and WW domain (lower domain); however, the R14A mutant Pin1 does not bind phospho-peptides in the WW domain. The Pin1 catalytic domain (oriented at the top) binds and isomerizes proline-directed phosphorylations while the WW domain (oriented at the bottom) binds generally more tightly *but does not isomerize* the same motifs. B) A "top-down" view of the catalytic site of Pin1 bound to Pintide shows how highly solvated and featureless this surface of the protein is. This is one attribute which challenges traditional approaches to inhibition. C) Key residues and their contacts with Pintide are shown. Some key interactions include coordination of the phosphate in the cationic groove (comprising Lys63, Arg68, and Arg69), hydrophobic packing of the pipecolate in the proline pocket, hydrophobic packing of the napthyl group on the hydrophobic shelf, and, to a lesser extent, some hydrogen bonding interactions between amide carbonyl and nitrogen elements with backbone and sidechain donors and acceptors, respectively. Interestingly, Pintide does not engage Arg68 which is involved in coordinating peptide mimics of known Pin1 substrates as well as other structurally characterized phosphorylated inhibitors of the Pin1 catalytic domain.

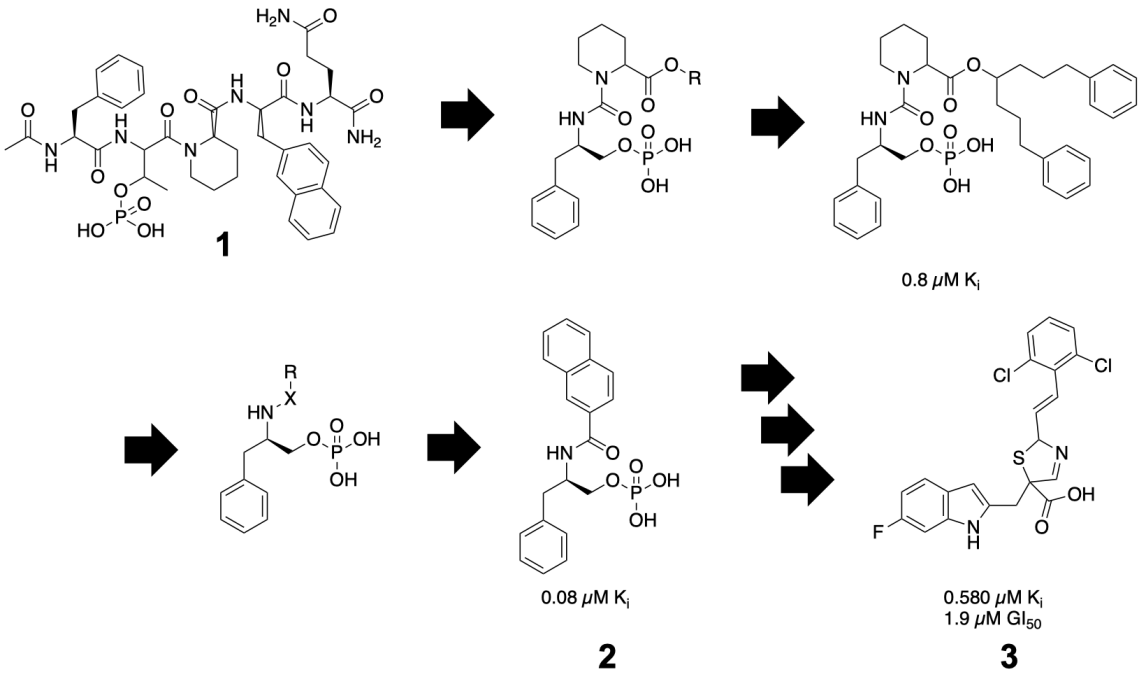

Figure 1.3. Pfizer development schematic exemplifies potency-permeability trade-off faced with traditional approaches to lead optimization. The structure-guided design of Pin1 inhibitors conducted by Guo and colleagues at Pfizer originated with Pintide (**1**). This molecule was reduced to key binding elements as outlined in Figure 1.2. High nanomolar binders were achievable even with highly flexible linkers and with a significant effort to reduce down to a reduced scaffold, low nanomolar binders such as **2** were achieved. While **2** is a potent binder of Pin1, the retention of the phosphate made for a complete lack of cellular activity. Interestingly, exchanging the phosphate in **2** with more bioavailable isosteres resulted in precipitous loss of affinity and reportedly still lacked activity in cell assays. Indeed, further rigidification and reduction of total polar surface area was necessary for achieving some biological activity and potency in the same molecule as shown in **3**. While these molecules were sufficient to show some bioactivity, they were apparently unsatisfactory to move forward.

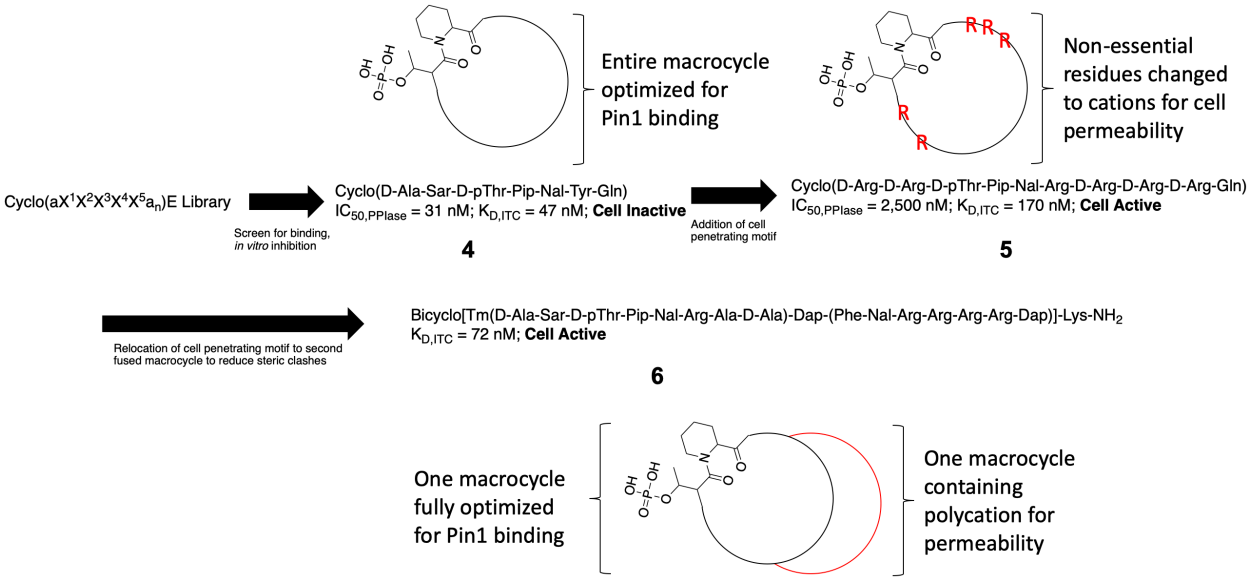

Figure 1.4. Development schematic of macrocyclic peptides for reversible competitive inhibition of Pin1 in cells. Macrocyclic peptides were first identified through a combinatorial library screen. Pin1 binding was detected by a fluorescence polarization assay in which a fluorescent Pin1 substrate peptide was competed off with candidate binders. Competitive inhibition was confirmed by re-testing of binders in a Pin1 PPIase activity assay. The most potent hits from the screen were used to design a molecule optimized for *in vitro* binding to Pin1 (**4**). In order to achieve cellular activity, **4** was modified by replacing residues which did not contribute appreciably to binding with cationic residues which are known to enhance active transport of otherwise impermeant molecules. While this molecule retained some *in vitro* potency and gained cellular permeability, the modifications of the core ring proved to be impactful on binding. To achieve both potent binding and cellular activity, investigators relocated the cell-penetrating motif (cationic residues) to an auxiliary ring which presumably does not interact with Pin1. Upon optimization of these molecules, the lead molecule **6** was highly permeant while being essentially equipotent in *in vitro* binding experiments to the affinity-optimized **4**.

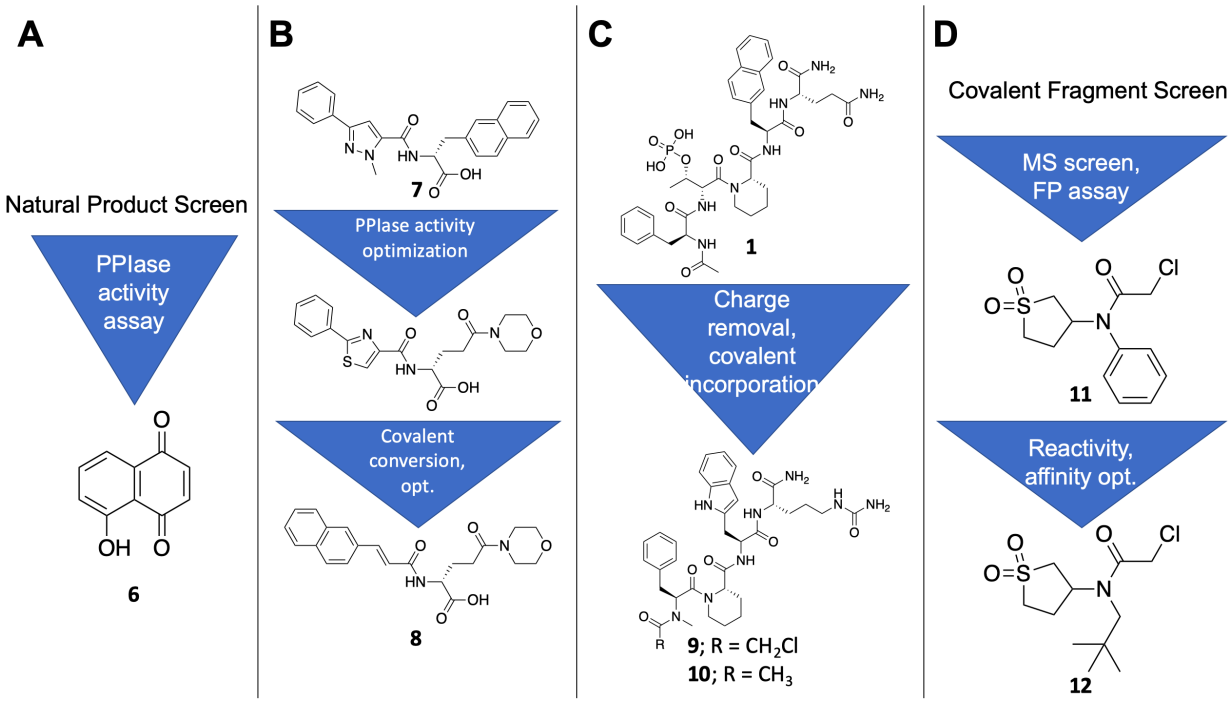

Figure 1.5. History of covalent inhibition of Pin1. A) The first molecule to reportedly inhibit Pin1, juglone (here, **6**) was discovered in a natural product screen for inhibitors of Pin1 catalysis. **6** which is isolated from black walnuts, covalently modifies the catalytically required Cys113 due to its uniquely low pKa and consequent nucleophilicity. Interestingly, **6** binds many highly reactive cysteines in the proteome. B) The first rationally designed covalent inhibitors of Pin1 started with the molecule **7** from a Vernalis medicinal chemistry effort and first further optimized for potent inhibitory activity. Following potency optimization, a Michael acceptor was engineered into the molecule. The lead molecule **8** labeled Pin1 with 1-to-1 stoichiometry and had some cellular activity. C) The most recent structure-based design of a Pin1 covalent inhibitor started with **1** which lacks cellular activity due to the anionic phosphate. Investigators removed the phosphate and installed an electrophilic chloromethyl amide in position proximal to C113 based on the binding pose observed in the co-crystal structure of **1**. The resultant molecule **9** was membrane permeant and potent relying on covalent modification for activity as demonstrated by the control molecule **10**. D) The most recent covalent inhibitor of Pin1 was discovered through a covalent fragment screen. After screening a large library of covalent fragments, cyclic sulfones were enriched as hits – a unique enrichment to Pin1. After some optimization of the original hit **11**, slight improvements on affinity were made. Additionally, of a small library of Pin1 binders based around **11**, **12** was the only molecule which did not induce non-specific toxicity in fibroblasts. **12** was demonstrated to be active in cells and in mice where in the spleen and in blood cells target engagement was validated.

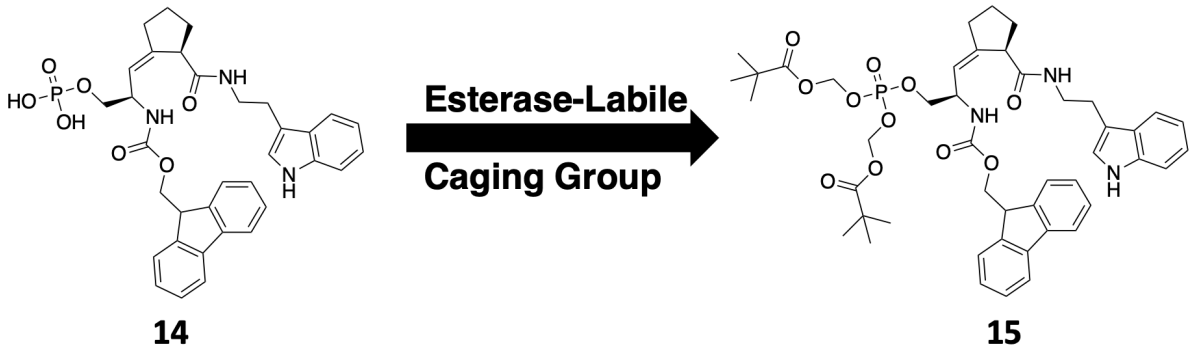

14 **15**

Figure 1.6. Bis-POM phosphate prodrugs for the *in cellulo* inhibition of Pin1. The first Pin1 prodrug was designed starting with **14** and caging it with Bis-POM esterase-labile groups. This caging moiety, following esterase cleavage hydrolyzes to the parent phosphate in cells. The investigators go on to show some level of proof of concept for improved activity in cells; however, target engagement and validation of a Pin1-dependency in their biomarker for activity were not demonstrated.

CHAPTER 2

DESIGN AND SYNTHESIS OF NON-NUCLEOTIDE PHOSPHORAMIDATE PIN1 INHIBITORS

Daniel MC Schwarz, Sarah K Williams, Jason E Gestwicki

Background. Phosphate groups are important in molecular recognition throughout biology. However, inhibitors that incorporate phosphates or phospho-mimetics are often too anionic to be passively permeable to biological membranes (1–3). Accordingly, many prodrug strategies have been developed to mask phosphates (4–6), allowing better balance between potency, selectivity and permeability. One of the most successful of these prodrug approaches is the phosphoramidate-based "ProTide" technology (7). This caging group relies on the consecutive action of esterase activity on the *O*-carboxy ester, followed by liberation of the phospho-ester by intramolecular nucleophilic attack, and then hydrolysis of the *N*-linked amino ester by a intracellular phosphoramidase, often the histidine triad nucleotide binding protein 1 (Hint1) (8). Together, these activities deliver the active, phosphate-bearing molecule to the cytosol. ProTide approaches have proven especially successful in enhancing the cellular delivery of nucleotide-based anti-virals, including blockbuster drugs (*i.e.* sofosbuvir (9,10)), clinical candidates (*i.e.* NUC-1031 (11)), and tool molecules (*i.e.* 4Ei-10 (12)). However, the applicability of ProTide technology to non-nucleotides is nascent; while phosphoramidates have been shown to improve the plasma lifetime and clogP values for a handful of non-nucleotides(13–16), it is not yet clear whether they can be enzymatically liberated in cells (Figure 2.1). Indeed, Hint1 is a selective, metabolic enzyme, which might not be considered likely to accept non-nucleotides that are structurally distinct from its natural substrates. Crystal structures of substrate-bound Hint1 have supported this idea, revealing a restrictive substrate envelope that is dominated by polar interactions around the phosphate (8). However, we noted that an adjacent, hydrophobic pocket, which is normally involved in accommodating the nucleobase, was potentially more amenable to alternative substrates. A search of appropriate, phosphate-containing inhibitors in the literature turned our attention to inhibitors of the peptidyl-prolyl isomerase, Pin1.

Pin1 is considered an attractive cancer target, owing to its high expression in breast and prostate tumors and the strong anti-tumor effects of Pin1 knockdown (17). Pin1 is a two-domain protein composed of a catalytic peptidyl-prolyl isomerase domain and non-catalytic WW domain. Both of these domains bind selectively to prolines that are adjacent to phosphorylated Ser/Thr (*e.g.* the pS/T-Pro motif). Only the catalytic domain, however, can isomerize this bond, facilitating interconversion between *cis* and *trans* peptidyl-prolyl bonds (18). Potent inhibitors of Pin1's catalytic activity, such as **2** (Figure 1.3), were described by Pfizer and the phosphate was found to impart significant affinity, but these molecules were too polar to be membrane permeable (19). Attempts to improve these compounds focused on replacing the phosphate and optimizing non-polar contacts (19–23). Alternatively previous work has also overcome poor permeability of phosphate-baring Pin1 inhibitors using bis-POM masking groups (24). Likewise, cyclic peptides (25) and covalent inhibitors lacking the phosphate, have been explored (26,27). While these efforts yielded important insights into the potential of Pin1 as a drug target, we envisioned a complementary approach, in which ProTide technology might be used to increase the permeability of Pfizer's molecules.

Design of Non-Nucleotide, Hint1-Liberated Phosphoramidate Pin1 Inhibitors.

The liberation of phosphoramidate prodrugs in the cell is mediated through two enzymatic reactions (Figure 2.1). Briefly, the carboxyester is first liberated by a carboxyesterase (i.e. CES1). The free carboxylate then attacks the phosphate core substituting the aromatic ester by an intramolecular S_N2 mechanism. The cyclic intermediate is hydrolyzed leaving the stable intermediate phosphoramidate. This intermediate is then a substrate for the phosphoramidase class of enzymes (i.e. Hint1) leading to the desired parent phosphate.

Importantly, Hint1 is an enzyme with a physiological role in liberating nucleotide phosphoramidates and previously had only been shown in the literature to liberate nucleotide analogs; however, it's likely that the phosphoramidase Hint1 may accommodate non-nucleotide phosphoramidates given the molecule fits in the substrate pocket (Figure 2.2A). Given this constraint, highly ligand-efficient Pin1 inhibitors were selected and hypothetical phosphoramidate analogs were curated by *in silico* docking experiments (Figure 2.2B). These experiments showed reasonable binding poses of the hypothetical phosphoramidates **16-(*R/S*)** in the Hint1 active site. Further analysis revealed that the binding energies of **16-(*R/S*)** were comparable to the known Hint1 substrate **sofosbuvir-Ala** – the intermediate metabolite of the clinical drug sofosbuvir. Importantly, no significant differences were observed between both each possible diastereomer of **16-(*R*)** or **16-(*S*)** metabolites (Figure 2.2E).

These results suggest that assuming the prodrug was permeant and carboxyesterase-labile, that these prodrugs would be converted into the active parent phosphate readily in human cells. Importantly, the parent of **16-(*R/S*)** (**17**) has a reported K_i of 150 nM against the isolated catalytic domain of Pin1. This makes it among the most potent inhibitors to be reported for Pin1 and an exceptional starting point for the development of selective Pin1 inhibitors if effectively delivered to cells.

Synthesis of Phosphate and Phosphoramidate Pin1 Inhibitors. To evaluate the effect of inhibiting Pin1 in cells, phosphate (**17**) and phosphoramidate (**16**) analogs were synthesized in each enantiomer (Figure 2.3). The (*R*) and (*S*) enantiomers of **17** were predicted to bind with significantly different affinities given the crystallographic data available (Figure 2.4) so **17-** and **16-(*S*)** were synthesized as control molecules for *in vitro* and *in vivo* experiments respectively.

Compounds **17-(*R/S*)** were synthesized first using simple amide coupling chemistry to form intermediates **d-(*R/S*)** followed by a single step phosphorylation recently published for the conversion of aliphatic hydroxyls directly to their corresponding phosphates (28). These conditions avoided any possible epimerization and were easily purified by semi-preparative HPLC.

The synthesis of compounds **16-(*R/S*)** began with the telescoped synthesis of racemic phosphoramoyl chloride **b** using chemistry developed for the manufacture of sofosbuvir (29). This intermediate was carried on to react crude with intermediates **d-(*R/S*)** to produce the diastereomeric mixture for each **16-(*R*)** and **16-(*S*)**. These molecules were used in diastereomeric mixture (~1:1) for simplicity as preliminary docking experiments do not suggest a bias for the binding of one diastereomer or another to the Hint1 catalytic domain. Therefore, the nomenclature of (*R*) and (*S*) refers only to the carbon stereocenter present alpha to the amide in the core of the molecules.

***In Vitro* Evaluation of Pin1 Binding.** Based on co-crystal structures, we anticipated that **17-(*R*)** would bind Pin1, while **17-(*S*)** would be an important, inactive control. To test this idea, we measured binding to the purified catalytic domain of human Pin1 (Pin1-Cat; residues 45 – 163, Figure 2.5A) by fluorescence polarization (FP) . In these experiments, we estimated inhibition constant (IC_{50}) values, based on competition with a fluorescent peptide FITC-WFYpSPFLE (PinTide) that is known to bind and inhibit the Pin1 catalytic site. As expected, we found that the **17-(*R*)** (IC_{50} <300 nM), but not **17-(*S*)** (IC_{50} >10,000 nM), bound to Pin1-Cat. Further, we confirmed that neither of the pro-drugs, **16-(*R/S*)**, were able to bind Pin1-Cat (IC_{50} > 10,000 nM). (Figure 2.5B)

Having confirmed that **17-(*R*)** binds the catalytic site, we turned to studying the full-length protein (Pin1-FL, Figure 2.5A). As mentioned above, Pin1-FL also contains a non-catalytic WW domain, which has been shown to bind phosphorylated peptides containing a *trans*-proline (30). We expected that **17-(*R*)** might be selective for the catalytic site over the WW domain, because it mimics the twisted-amide transition state that is only preferred by that site (19,31). Indeed, using isothermal titration calorimetry (ITC), we found that **17-(*R*)** bound Pin1-FL with a stoichiometry ~1 (N = 0.94 ± 0.03), suggesting that it primarily interacts with the catalytic site. We also noticed that a dissociation constant (K_d) of **17-(*R*)** for Pin1-FL (72 ± 37 nM) was enhanced over the value measured for binding the truncated Pin1-Cat (Figure 2.6C); an improvement that was expected because similar effects have been previously observed for Pin1 substrates (32). Together, these binding studies showed that **17-(*R*)** (but not **17-(*S*)** or **16-(*R/S*)**) binds Pin1 with the expected affinity and domain preference *in vitro*.

***In Vitro* and *In Cellulo* Analysis of Permeability.** Permeability of phosphates is hindered by their physicochemical properties. Namely, the charge of the phosphate hinders solubility in the lipid bilayer of the cell membrane and also reduces the effective concentration of the molecule at the cell surface by coulombic forces. Therefore, we tested these physicochemical properties – relative hydrophobicity and permeability – of **17-(*R*)** and **16-(*R*)**. As predicted by calculations, in octanol-water partitioning (a measure of hydrophobicity), the phosphoramidate was determined to be significantly more hydrophobic than the phosphate (Figure 2.6A). Consistent with this difference, the phosphoramidate was also more permeable in a parallel artificial membrane assay (PAMPA) (Figure 2.6B).

Encouraged by this result, we then explored whether **16-(*R*)** might be enzymatically liberated to **17-(*R*)** in cells. To ask test this, K562 cells were treated for five hours under serum-free conditions, followed by extensive washing, centrifugation, ethyl acetate extraction and measurement of the reaction products by ultra-high-performance liquid chromatography mass spectrometry (UPLC-MS) (Figure 2.7). Satisfyingly, both the intermediate product of esterase activity and the **17-(*R*)** product were detected in the treated K562 cell lysate. In addition, a small amount of the dephosphorylated metabolite was also present and its identity confirmed with an authentic standard. The free phosphate peak increased with time, consistent with enzymatic turnover. To ensure that **17-(*R*)** was indeed being processed by intracellular enzymes, we repeated the extractions in media lacking cells. In these controls, neither the intermediate nor **17-(*R*)** were identified, confirming that enzymatic activity was required. Together, these results suggest that **16-(*R*)** is cell-permeable and that it is converted to its active form in cells.

Validation of Target Engagement in Cells. The next question is whether the liberated **17-(*R*)** might engage Pin1. Due to the low permeability of **17-(*R*)** itself, this question could not previously be addressed. To test it, we performed a cellular thermal shift assay (CETSA). Specifically, K562 cells were treated with **16-(*R*)** (25 μM) or solvent alone (0.25% DMSO) for 5 hours to allow for liberation of the active molecule. Then, cells were heated on a temperature gradient, lysed, and the soluble fraction assayed for Pin1 abundance by western blot. We found that Pin1 was partially protected by the compound treatment, consistent with binding of **17-(*R*)** to Pin1 (Figure 2.8A). This result was also repeated in MDA-MB-231 cells, a model of metastatic breast cancer (Figure 2.8B). This experiment was important because Pin1 has been specifically implicated in both prostate and breast cancers (17). In these experiments, we leveraged the findings from the K562 studies and performed the CETSA near the most sensitive, half-maximal temperature (48

˚C). As in the K562 cells, Pin1 was stabilized. Together, these results suggest that **17-(*R*)** is released from **16-(*R*)** and that it binds Pin1 in two cancer cell types.

Support and Validation of a Hint1-Mediated Liberation Mechanism. While the cell-dependent observation of the parent molecule **17-(*R*)** accumulating over time was convincing that the molecule was being converted in cells, the dependence on the canonical enzyme, Hint1, was unknown. To test the dependence on Hint1, a chemical Hint1 inhibitor TrpGc (33–35) was used in combination with **16-(*R*)** and perturbation of Pin1 target engagement was evaluated. In early experiments, we had noticed that, at timepoints longer than 24 hours, treatment of various cell types (i.e. MDA-MB-231) with **16-(*R*)** but not **16-(*S*)** or **17-(*R*)** led to a dose-responsive increase in Pin1 levels, even at physiological temperatures (Figure 2.6B). Using this biomarker, we found that co-treatment with TrpGc (100 μM) blocked the cellular activity of **16-(*R*)**, supporting an essential role for Hint1 in uncaging (Figure 2.9).

Together, these results suggest that **16-(*R*)** is liberated by Hint1 in cells, releasing **17-(*R*)**, which then binds Pin1's catalytic site and inhibits some of its functions. Thus, we propose that **16-(*R*)** will be a useful chemical tool, enabling future studies into Pin1's enigmatic roles in cancer. Such future studies would also benefit from understanding which phosphoramidate diastereomer is a better substrate for Hint1, as well as quantitative measurements of its cytosolic conversion kinetics.

More broadly, this work provides initial evidence that the "ProTide" approach is more broadly applicable than previously appreciated. We speculate that additional evaluation of Hint1's substrate envelope might open this approach to additional scaffolds. For example, molecular recognition in kinase/phosphatase signaling, 14-3-3 scaffolding and nucleoside

metabolism involves selective binding of phosphates (36). As envisioned, this pro-drug approach re-balances the interplay between permeability and potency, allowing chemical probes to include the natural phosphate that is so important in molecular recognition.

Materials and Methods:

Synthesis intermediate b: In a flask equipped with a drying column and argon balloon, phosphorous(V)oxychloride (1.0 eq) and phenol (1.0 eq) were dissolved in anhydrous DCM and sparged with Ar gas for 5 minutes while stirring at ambient temperature. The reaction mixture was cooled to -78 ˚C and anhydrous diisopropylethylamine amine (DIPEA) (1.5 eq) was added dropwise. The mixture was stirred at -78 ˚C for 30 minutes and then allowed to slowly warm to ambient temperature. After stirring at ambient temperature for 2 hours, the mixture was concentrated by rotary evaporation with drying column adapter and resuspended in anhydrous diethyl ether. White precipitate was filtered under a blanket of Ar gas. Flow-through was once again concentrated by rotary evaporation under a drying column and resuspended in anhydrous DCM. To the solution was added ethyl glycine hydrochloride (1.0 eq) and the solution was sparged with Ar gas for 5 minutes at ambient temperature. The reaction mixture was cooled to -78 ˚C and DIPEA (3.0 eq) was added dropwise. Resultant mixture was stirred at -78 ˚C for 30 minutes and allowed to slowly warm to ambient temperature. Following a 2-hour incubation, the mixture was concentrated to dryness on a rotary evaporator under a drying column. The residue was resuspended in diethyl ether and white solids were filtered under a blanket of argon. Flow through was concentrated to dryness and resuspended in anhydrous THF. Crude was carried forward without characterization and used immediately.

Synthesis of the enantiomers of intermediate d: To a flask charged with D- or L-phenylglycinol (1.0 eq) and benzo[*b*]thiophene-2-carbonyl chloride (1.2 eq) was added anhydrous tetrahydrofuran and DIPEA (2.5 eq). The reaction mixture was stirred at ambient temperature overnight. The reaction mixture was diluted in EtOAc and washed with 2 × 0.5M HCl (aqueous) then 3 × brine. The organic layer was dried with sodium sulfate and concentrated to dryness. The resultant residue was purified by flash column chromatography (silica gel 0-20% methanol in dichloromethane).

Intermediate d-(*R*): ^{1}H-NMR (d_6-DMSO, 400 MHz) δ: 8.53 (d, *J*=0.02, 1H), 8.13 (s, 1H), 8.04 – 7.90 (m, 2H), 7.50 – 7.39 (m, 2H), 7.32 – 7.20 (m, 4H), 7.20 – 7.11 (m, 1H), 4.96 – 4.88 (m, 1H), 4.21 – 4.09 (m, 1H), 3.59 – 3.42 (m, 2H), 3.01 – 2.75 (m, 2H). ^{13}C-NMR (d_6-DMSO, 400 MHz) δ:161.57, 140.77, 140.56, 139.74, 139.62, 129.55, 128.63, 126.55, 126.40, 125.58, 125.32, 124.98, 123.22, 63.25, 54.00, 36.92; Molecular formula: $C_{18}H_{17}NO_2S$; ESI-MS $[M+H]^+$: Expected: 312.11, Observed: 312.71; ≥95% purity by UPLC. Yield: 213 mg, 41%.

Intermediate d-(*S*): ^{1}H-NMR (d_6-DMSO, 400 MHz) δ: 8.53 (d, *J*=0.02, 1H), 8.13 (s, 1H), 8.03 – 7.90 (m, 2H), 7.49 – 7.38 (m, 2H), 7.33 – 7.21 (m, 4H), 7.20 – 7.12 (m, 1H), 4.92 (t, *J*= 0.02, 1H), 4.21 – 4.08 (m, 1H), 3.57 – 3.42 (m, 2H), 3.01 – 2.75 (m, 2H). ^{13}C-NMR (d_6-DMSO, 400 MHz) δ:161.57, 140.75, 140.55, 139.72, 139.63, 129.54, 128.61, 126.53, 126.40, 125.56, 125.32, 124.98, 123.22, 63.25, 54.00, 36.92; Molecular formula: $C_{18}H_{17}NO_2S$; ESI-MS $[M+H]^+$: Expected: 312.11, Observed: 312.62; ≥95% purity by UPLC. Yield: 262 mg, 50%.

Synthesis of 16-(*R*) and 16-(*S*): intermediate **d** (1.0 eq) was dissolved in anhydrous THF and sparged with Ar gas. To the solution was added 1.0 M tert-butyl magnesium chloride dropwise (1.2 eq) and the resultant mixture was stirred at room temperature for 30 min. Intermediate **b** (crude, excess) was added to the slurry dropwise and the resultant reaction mixture was stirred at ambient temperature overnight. The mixture was concentrated to residue and purified by reverse-phase flash chromatography to a 55:45 mixture of diastereomers by UPLC (C18 5 - 95% acetonitrile in water).

Compound 16-(*R*): ^{1}H-NMR (d_6-DMSO, 400 MHz) δ: 8.73 (d, J=0.02, 1H), 8.10 (d, J=0.01, 1H), 7.99 (dd, J_{ba}=0.05, J_{bc}=0.02, 2H), 7.46 (m, 2H), 7.25 (m, 10H), 5.94 (q, J=0.18, 1H), 4.39 (m, 1H), 4.10 (m, 2H), 4.01 (m, 2H), 3.66 (q, J=0.02), 2.90 (m, 2H), 1.12 (m, 3H). ^{13}C-NMR (d_6-DMSO, 400 MHz) δ:171.22, 161.76, 161.70, 151.14, 140.60, 140.24, 139.50, 138.62, 130.05, 129.97, 129.54, 128.73, 126.74, 126.68, 125.58, 125.39, 125.23, 125.03, 124.96, 123.26, 120.75, 120.70, 60.91, 42.83, 14.43; Molecular formula: $C_{28}H_{29}N_2O_6PS$; ESI-MS $[M+H]^+$: Expected: 553.16, Observed: 552.28; ≥95% purity by UPLC (54:46 diastereomeric ratio). Yield: 105 mg, 60%.

Compound 16-(*S*): ^{1}H-NMR (d_6-DMSO, 400 MHz) δ: 8.74 (d, J=0.02, 1H), 8.10 (d, J=0.01, 1H), 7.99 (dd, J_{ba}=0.05, J_{bc}=0.02, 2H), 7.46 (m, 2H), 7.25 (m, 10H), 5.94 (q, J=0.18, 1H), 4.39 (m, 1H), 4.10 (m, 2H), 4.01 (m, 2H), 3.66 (q, J=0.02), 2.90 (m, 2H), 1.12 (m, 3H). ^{13}C-NMR (d_6-DMSO, 400 MHz) δ:171.21, 161.76, 161.70, 140.64, 140.24, 139.54, 138.67, 130.05, 129.98, 129.54, 128.72, 126.71, 126.66, 125.61, 125.39, 125.23, 125.03, 124.97, 123.27, 120.74, 120.69, 60.92, 42.93, 14.42; Molecular formula: $C_{28}H_{29}N_2O_6PS$; ESI-MS $[M+H]^+$: Expected: 553.16, Observed: 552.64; ≥95% purity by UPLC (57:43 diastereomeric ratio). Yield: 94 mg, 54%.

Synthesis of compound 17-(*R*) and 17-(*S*): Intermediate **d** (1.0 eq), phospho(enol)pyruvic acid mono potassium salt (10.0 eq), and tetrabutylammonium hydrogen were dissolved in anhydrous dimethylformamide and sparged with Ar gas. The mixture was heated to 100 ˚C and stirred under Ar gas for 5 hours. The mixture was purified by semi-preparative HPLC (C18 5 - 95% acetonitrile in water) (28).

Compound 17-(*R*): ^{1}H-NMR (MeOD, 400 MHz) δ: 7.98 (s, 1H), 7.90 – 7.87 (m, 2H), 7.48 – 7.40 (m, 2H), 7.37 -7.18 (m, 5H), 4.55 – 4.42 (m, 1H), 4.18 – 4.02 (m, 2H), 3.14 – 2.95 (m, 2H). ^{13}C-NMR (MeOD, 400 MHz) δ: 141.01, 139.33, 138.62, 137.83, 128.98, 128.11, 126.20, 126.05, 125.15, 124.82, 124.57, 122.15, 66.34, 51.98, 36.27; Molecular formula: $C_{18}H_{18}NO_5PS$; ESI-MS $[M+H]^+$: Expected: 392.07, Observed: 391.35; ≥95% purity by UPLC. Yield: 56 mg, 54%.

Compound 17-(*S*): ^{1}H-NMR (MeOD, 400 MHz) δ:7.97 (s, 1H), 7.95 – 7.86 (m, 2H), 7.49 – 7.38 (m, 2H), 7.37 -7.15 (m, 5H), 4.56 – 4.31 (m, 1H), 4.18 – 3.99 (m, 2H), 3.14 – 2.96 (m, 2H). ^{13}C-NMR (MeOD, 400 MHz) δ: 141.05, 139.36, 138.59, 137.83, 128.97, 128.11, 126.18, 125.99, 125.17, 124.84, 124.55, 122.14, 66.29, 51.96, 36.27; Molecular formula: $C_{18}H_{18}NO_5PS$; ESI-MS $[M+H]^+$: Expected: 392.07, Observed: 391.58; ≥95% purity by UPLC. Yield: 33 mg, 33%.

Protein expression and purification: The full length and catalytic constructs of Pin1 were expressed and purified as previously described (37).

Cell culture: MDA-MB-231 cells were obtained from American Type Culture Collection (ATCC) and cultured in Dulbecco's Modified Eagle's Medium (DMEM) supplemented with 10% fetal bovine serum and 100 µg/mL penicillin/streptomycin. K562 and PC3 cells were obtained by ATCC and cultured in Roswell Park Memorial Institute (RPMI) medium supplemented with 10% fetal bovine serum and 100 µg/mL penicillin/streptomycin. All cells were maintained at 37˚C and 5% CO_2 in a humidified incubator.

Pin1-cat competition fluorescence polarization: In a M5 plate reader (SpectroMax), competition experiments were conducted at a fixed concentration of Pin1-cat (500 nM) and fluorescent tracer peptide FITC-WFYpSPFLE (sometimes referred to as PinTide; 25 nM) and varying competitor competition. The $K_{i,app}$ values were calculated using the following equation (38):

$$K_{i,app} = I_{50}/(L_{50}/K_d + P_0/K_d + 1)$$

Where I_{50} is the concentration of free inhibitor at 50% inhibition, L_{50} is the concentration of free tracer at 50% inhibition, P_0 is the total receptor concentration, and K_d is the dissociation constant of receptor and tracer (3.53 µM).

Isothermal titration calorimetry (ITC): Affinity and stoichiometry of binding to the full length Pin1 were measured in a microCal ITC200 (General Electric). In these experiment, ligand (50 µM) in 0.5% DMSO 50 mM Tris, 50 mM NaCl, pH 7.5 was loaded into the syringe, while the cell was loaded with Pin1 (5 µM) in 0.5% DMSO, 50 mM Tris, 50 mM NaCl, pH 7.5. Isotherms measured during the titration were converted to their corresponding Wiseman plots using PEAQ-ITC analysis software (Malvern Panalytical).

Octanol/water partitioning: Each compound was diluted to 50 µM in deionized water and 0.5% DMSO. To a 500 µL volume of each solution, 250 µL of 1-octanol was added and the mixture was vortexed to an emulsion. The emulsions were left to separate at ambient temperature for four hours. Following separation, absorbance measurements for each phase were taken at 250 nm wavelength. The A_{250} for each phase was compared to solvent-matched standard curves to determine the concentration of either **17-(*R*)** or **16-(*R*)**. Partitioning coefficient was determined using the following formula:

$$log_{10}P = log_{10}\left(\frac{[compound]_{4\ hours}}{34\ \mu M}\right)$$

Parallel artificial membrane permeability assay: PAMPA assays were conducted per the manufacturer's instructions (Sigma Aldrich). Briefly, each compound was diluted to 50 µM in PBS (pH 7.4, Gibco) and 0.5% DMSO. This solution (150 µL) was added to a PVDF membrane filter plate (Sigma Aldrich) coated with 5 µL phosphatidyl choline in dodecane (20 mg/mL). The filter plate was inserted into an acceptor plate with 300 µL PBS with 0.5% DMSO and incubated for 16 hours. Following incubation, A_{250} was recorded for each acceptor well and concentrations were determined using a solvent-matched standard curve. Permeability rates were determined using the following equation:

$$log_{10}Pe = log_{10}\left\{C\left(-\ln\left(1-\frac{[compound]_{acceptor}}{34\ \mu M}\right)\right)\right\}$$

For the apparatus and volumes specified above C is $1.16*10^{-4}$.

Cellular liberation of phosphate by LC-MS: K562 cells at a density of 3.9 million cells per milliliter were treated with **16-(*R*)** in serum free conditions for 5 hours. Following incubation, 1 mL of cell suspension was pelleted at 300 relative centrifugal force. The

media was removed and pellets were then resuspended in 1 mL ethyl acetate and incubated at -30 ˚C for 24 hours. Following extraction, the mixture was concentrated by rotary evaporation and the residue was resuspended in LC-MS grade methanol (100 µL). The resultant solution was filtered and analyzed on an Acquity H-Class/TQD UPLC-MS/MS (Model #: B10UPB541M; Waters). Purified standards of **16-(R)**, **17-(R)**, and intermediate **d** elution times and m/z were compared to the LC-MS trace of cell extract and appreciable **17-(R)** and **16-(R)** were detected with trace intermediate **d** detected. In the time course experiment, the AUC of the peak corresponding to the **17-(*R*)** •Na mass was quantified.

Cellular thermal shift assay (CETSA): K562 cells were treated with **16-(R)** (25 µM) or matching concentration of DMSO for 5 hours and incubated under standard growth conditions (37 ˚C, 5% CO_2). Following incubation, cells were pelleted and resuspended in compound- or mock-treated media at a density of 2 million per mL. 50 µL aliquots were transferred to PCR tubes and were heated to a set temperature from 38 – 60 ˚C (at 2 ˚C increments) for 4 minutes. Tubes were then returned to ambient temperature for 4 minutes and then snap-frozen in liquid nitrogen. Cells were lysed by freeze-thaw cycles (3) and the insoluble fraction was pelleted by high-speed centrifugation. Soluble fractions were assayed by western blot for Pin1 and tubulin. MDA-MB-231 cells were treated under standard growth conditions with 25 µL **16-(*R*)** or matching concentration of DMSO for 5 hours. Cells were lifted by mechanical scraping, pelleted, and resuspended to a density of 2 million per mL. Cell slurry was portioned to 50 µL aliquots and were heated to 48 ˚C for 4 minutes. Slurry was then cooled to ambient temperature for 4 minutes and snap frozen in liquid nitrogen. Samples were processed and analyzed as described for K562 samples.

Pin1 induction assay: MDA-MB-231 cells were treated with **16-(*R*)** or DMSO for 72 hours and were subsequently lysed in 4% SDS in TBS and boiled. Clarified lysate was assayed by western blot for Pin1 and tubulin. Subsequently, MDA-MB-231 cells were treated with 5 μM **16-(*R*)** or **16-(*S*)**, 5 μM **16-(*R*)** with 100 μM TrpGc, or 100 μM TrpGc alone for 48 hours. Cells were subsequently lysed, lysate was clarified and assayed by western blot for Pin1 and tubulin (as above).

Hint1 docking experiments:

The Hint1 co-crystal structure bound to 5'-O-[(L-lysylamino)sulfonyl]adenosine (Accession: 4EQE) was submitted for docking experiments in SwissDock (39) with all four diastereomers of compound 18-(*R*) as well as a sofosbuvir-alanine positive control.

Mol2 models of each compound were prepared at a simulated pH 7.0 in Open Bable (40) and were each submitted to identical docking experiments with default settings in SwissDock. Resultant poses were manually curated for approximately proper pose in the catalytic pocket for hydrolysis and energy scores and $\Delta G_{binding}$ were plotted in Prism 8 (Graphpad). Structures were overlaid with the co-crystal structure to evaluate the orientation of the lowest energy poses.

References

1. Lipinski CA. Drug-like properties and the causes of poor solubility and poor permeability. J Pharmacol Toxicol Methods. 2000;44(1):235–49.
2. Palte MJ, Raines RT. Interaction of nucleic acids with the glycocalyx. J Am Chem Soc. 2012;134(14):6218–23.
3. Leeson PD, Springthorpe B. The influence of drug-like concepts on decision-making in medicinal chemistry. Nat Rev Drug Discov. 2007;6(11):881–90.
4. Gross DM, Sweet CS, Ulm EH, Backlund EP, Morris AA, Weitz D, et al. Effect of N-[(S)-1-carboxy-3-phenylpropyl]-L-Ala-L-Pro and its ethyl ester (MK-421) on angiotensin converting enzyme in vitro and angiotensin I pressor responses in vivo. J Pharmacol Exp Ther. 1981;216(3):552–7.
5. Tsien RY. A non-disruptive technique for loading calcium buffers and indicators into cells. Nature. 1981;290(5806):527–8.
6. McGuigan C, Devine KG, O'Connor TJ, Kinchington D. Synthesis and anti-HIV activity of some haloalkyl phosphoramidate derivatives of 3′-azido-3′-deoxythymidine (AZT): potent activity of the trichloroethyl methoxyalaninyl compound. Antiviral Res. 1991;15(3):255–63.
7. Curley D, McGuigan C, Devine KG, O'Connor TJ, Jeffries DJ, Kinchington D. Synthesis and anti-HIV evaluation of some phosphoramidate derivatives of AZT: Studies on the effect of chain elongation on biological activity. Antiviral Res. 1990;14(6):345–56.
8. Maize KM, Shah R, Strom A, Kumarapperuma S, Zhou A, Wagner CR, et al. A Crystal Structure Based Guide to the Design of Human Histidine Triad Nucleotide Binding Protein 1 (hHint1) Activated ProTides. Mol Pharm. 2017;14(11):3987–97.
9. Sofia MJ, Bao D, Chang W, Du J, Nagarathnam D, Rachakonda S, et al. Discovery of a luoro-2′-β- C -methyluridine Nucleotide Prodrug (PSI-7977) for the treatment of hepatitis C virus. J Med Chem. 2010;53(19):7202–18.
10. Murakami E, Tolstykh T, Bao H, Niu C, Micolochick Steuer HM, Bao D, et al. Mechanism

of activation of PSI-7851 and its diastereoisomer PSI-7977. J Biol Chem. 2010;285(45):34337–47.

11. Blagden SP, Rizzuto I, Suppiah P, O'Shea D, Patel M, Spiers L, et al. Anti-tumour activity of a first-in-class agent NUC-1031 in patients with advanced cancer: results of a phase I study. Br J Cancer [Internet]. 2018;119(7):815–22. Available from: http://dx.doi.org/10.1038/s41416-018-0244-1
12. Ahmad Z, Jacobson BA, McDonald MW, Vattendahl Vidal N, Vattendahl Vidal G, Chen S, et al. Repression of oncogenic cap-mediated translation by 4Ei-10 diminishes proliferation, enhances chemosensitivity and alters expression of malignancy-related proteins in mesothelioma. Cancer Chemother Pharmacol [Internet]. 2020;85(2):425–32. Available from: https://doi.org/10.1007/s00280-020-04029-9
13. Serpi M, Bibbo R, Rat S, Roberts H, Hughes C, Caterson B, et al. Novel phosphoramidate prodrugs of N-acetyl-(d)-glucosamine with antidegenerative activity on bovine and human cartilage explants. J Med Chem. 2012;55(10):4629–39.
14. Lentini NA, Foust BJ, Hsiao CHC, Wiemer AJ, Wiemer DF. Phosphonamidate Prodrugs of a Butyrophilin Ligand Display Plasma Stability and Potent V9 VÎ2 T Cell Stimulation. J Med Chem. 2018;61(19):8658–69.
15. Davey MS, Malde R, Mykura RC, Baker AT, Taher TE, Le Duff CS, et al. Synthesis and Biological Evaluation of (E)-4-Hydroxy-3-methylbut-2-enyl Phosphate (HMBP) Aryloxy Triester Phosphoramidate Prodrugs as Activators of Vγ9/Vδ2 T-Cell Immune Responses. J Med Chem. 2018;61(5):2111–7.
16. Miccoli A, Dhiani BA, Mehellou Y. Phosphotyrosine prodrugs: design, synthesis and anti-STAT3 activity of ISS-610 aryloxy triester phosphoramidate prodrugs. Medchemcomm [Internet]. 2019;10(2):200–8. Available from: http://dx.doi.org/10.1039/C8MD00244D
17. Shen M, Stukenberg PT, Kirschner MW, Lu KP. The essential mitotic peptidyl-prolyl isomerase Pin1 binds and regulates mitosis-specific phosphoproteins. Genes Dev.

1998;12(5):706–20.

18. Zhang M, Wang XJ, Chen X, Bowman ME, Luo Y, Noel JP, et al. Structural and kinetic analysis of prolyl-isomerization/phosphorylation cross-talk in the CTD code. ACS Chem Biol. 2012;7(8):1462–70.

19. Guo C, Hou X, Dong L, Dagostino E, Greasley S, Ferre R, et al. Structure-based design of novel human Pin1 inhibitors (I). Bioorganic Med Chem Lett [Internet]. 2009;19:5613–6. Available from: http://dx.doi.org/10.1016/j.bmcl.2009.08.034

20. Dong L, Marakovits J, Hou X, Guo C, Greasley S, Dagostino E, et al. Structure-based design of novel human Pin1 inhibitors (II). Bioorganic Med Chem Lett. 2010;20:2210–4.

21. Guo C, Hou X, Dong L, Marakovits J, Greasley S, Dagostino E, et al. Structure-based design of novel human Pin1 inhibitors (III): Optimizing affinity beyond the phosphate recognition pocket. Bioorganic Med Chem Lett [Internet]. 2014;24(17):4187–91. Available from: http://dx.doi.org/10.1016/j.bmcl.2014.07.044

22. Potter AJ, Ray S, Gueritz L, Nunns CL, Bryant CJ, Scrace SF, et al. Structure-guided design of α-amino acid-derived Pin1 inhibitors. Bioorganic Med Chem Lett [Internet]. 2010;20(2):586–90. Available from: http://dx.doi.org/10.1016/j.bmcl.2009.11.090

23. Potter A, Oldfield V, Nunns C, Fromont C, Ray S, Northfield CJ, et al. Discovery of cell-active phenyl-imidazole Pin1 inhibitors by structure-guided fragment evolution. Bioorganic Med Chem Lett [Internet]. 2010;20(22):6483–8. Available from: http://dx.doi.org/10.1016/j.bmcl.2010.09.063

24. Zhao S, Etzkorn FA. A phosphorylated prodrug for the inhibition of Pin1. Bioorganic Med Chem Lett. 2007;17(23):6615–8.

25. Liu T, Liu Y, Kao H-Y, Pei D. Membrane Permeable Cyclic Peptidyl Inhibitors against Human Peptidylprolyl Isomerase Pin1. J Med Chem [Internet]. 2010 Mar 25 [cited 2017 Mar 12];53(6):2494–501. Available from: http://pubs.acs.org/doi/abs/10.1021/jm901778v

26. Ieda N, Itoh K, Inoue Y, Izumiya Y, Kawaguchi M, Miyata N, et al. An irreversible inhibitor

of peptidyl-prolyl cis/trans isomerase Pin1 and evaluation of cytotoxicity. Bioorganic Med Chem Lett. 2019 Feb 1;29(3):353–6.

27. Dubiella C, Pinch BJ, Zaidman D, Manz TD, Poon E, He S, et al. Sulfopin , a selective covalent inhibitor of Pin1 , blocks Myc-driven tumor initiation and growth in vivo. bioRxiv [Internet]. 2020; Available from: https://doi.org/10.1101/2020.03.20.998443

28. Domon K, Puripat M, Fujiyoshi K, Hatanaka M, Kawashima SA, Yamatsugu K, et al. Catalytic Chemoselective O-Phosphorylation of Alcohols. ACS Cent Sci. 2020;6:283–92.

29. Serpi M, Madela K, Pertusati F, Slusarczyk M. Synthesis of phosphoramidate prodrugs: ProTide approach. Curr Protoc Nucleic Acid Chem. 2013;(SUPPL.53):1–15.

30. Rippmann JF, Hobbie S, Daiber C, Guilliard B, Bauer M, Birk J, et al. Phosphorylation-dependent proline isomerization catalyzed by Pin1 is essential for tumor cell survival and entry into mitosis. Cell Growth Differ [Internet]. 2000;11(7):409–16. Available from: http://www.ncbi.nlm.nih.gov/pubmed/10939594

31. Dunyak BM, Gestwicki JE. Peptidyl-Proline Isomerases (PPIases): Targets for Natural Products and Natural Product-Inspired Compounds. 2016;

32. Eichner T, Kutter S, Labeikovsky W, Buosi V, Kern D. Molecular Mechanism of Pin1-Tau Recognition and Catalysis. J Mol Biol [Internet]. 2016;428(9):1760–75. Available from: http://dx.doi.org/10.1016/j.jmb.2016.03.009

33. Bardaweel SK, Ghosh B, Wagner CR. Synthesis and evaluation of potential inhibitors of human and Escherichia coli histidine triad nucleotide binding proteins. Bioorganic Med Chem Lett [Internet]. 2012;22(1):558–60. Available from: http://dx.doi.org/10.1016/j.bmcl.2011.10.082

34. Shah RM, Peterson C, Strom A, Dillenburg M, Finzel B, Kitto KF, et al. Inhibition of HINT1 Modulates Spinal Nociception and NMDA Evoked Behavior in Mice. ACS Chem Neurosci. 2019;10(10):4385–93.

35. Okon A, Matos De Souza MR, Shah R, Amorim R, Da Costa LJ, Wagner CR.

Anchimerically Activatable Antiviral ProTides. ACS Med Chem Lett. 2017;8(9):958–62.

36. Hirsch AKH, Fischer FR, Diederich F. Phosphate recognition in structural biology. Angew Chemie - Int Ed. 2007;46(3):338–52.

37. Mok SA, Condello C, Freilich R, Gillies A, Arhar T, Oroz J, et al. Mapping interactions with the chaperone network reveals factors that protect against tau aggregation. Nat Struct Mol Biol [Internet]. 2018;25(5):384–93. Available from: http://dx.doi.org/10.1038/s41594-018-0057-1

38. Nikolovska-Coleska Z, Wang R, Fang X, Pan H, Tomita Y, Li P, et al. Development and optimization of a binding assay for the XIAP BIR3 domain using fluorescence polarization. Anal Biochem. 2004;332(2):261–73.

39. Grosdidier A, Zoete V, Michielin O. SwissDock, a protein-small molecule docking web service based on EADock DSS. Nucleic Acids Res. 2011;39:270–7.

40. O'Boyle NM, Banck M, James CA, Morley C, Vandermeersch T, Hutchison GR. Open Babel: An Open chemical toolbox. J Cheminform. 2011;3(10):1–14.

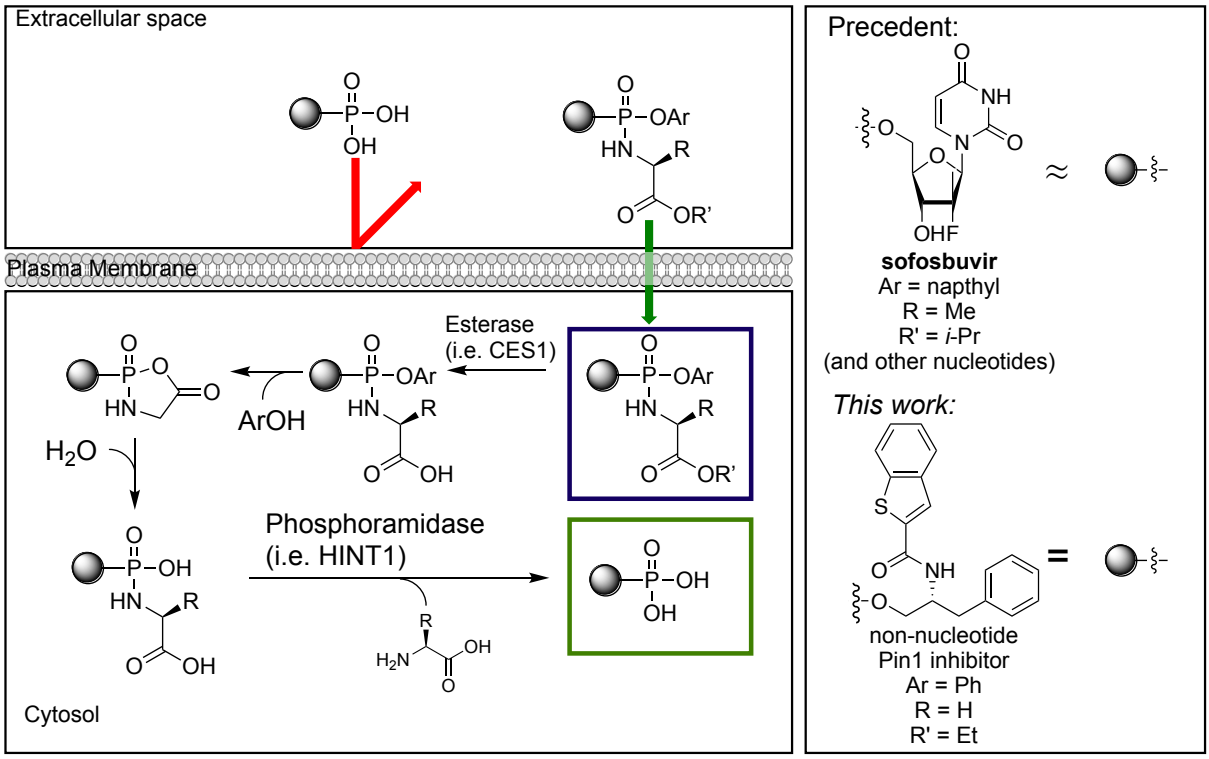

Figure 2.1. Adaptation of the phosphoramidate strategy for the delivery of Hint1 non-nucleotide phosphorylated parent molecules to cells. Previous work has demonstrated repeatedly that nucleotides and nucleotide analogs may be caged with aryloxy phosphoramidates and that these molecules are processed intracellularly by esterase and phosphoramidase enzymes. Importantly, the phosphoramidase responsible for the ultimate liberation step, Hint1, has physiological activity against nucleotide phosphoramidates. While previous non-nucleotide phosphoramidate prodrugs have been described in the literature (15,16), no clear evidence of liberation or testing of the mechanism of that liberation has been demonstrated. Here, we show clearly that Pin1 inhibitors are made cell permeable, processed into phosphate-baring parent molecule intracellularly, engage the target, and are dependent on the activity of Hint1 for their activity. To our knowledge this is the first example of a thorough investigation of non-nucleotide aryloxy phosphoramidate prodrugs in the literature to date.

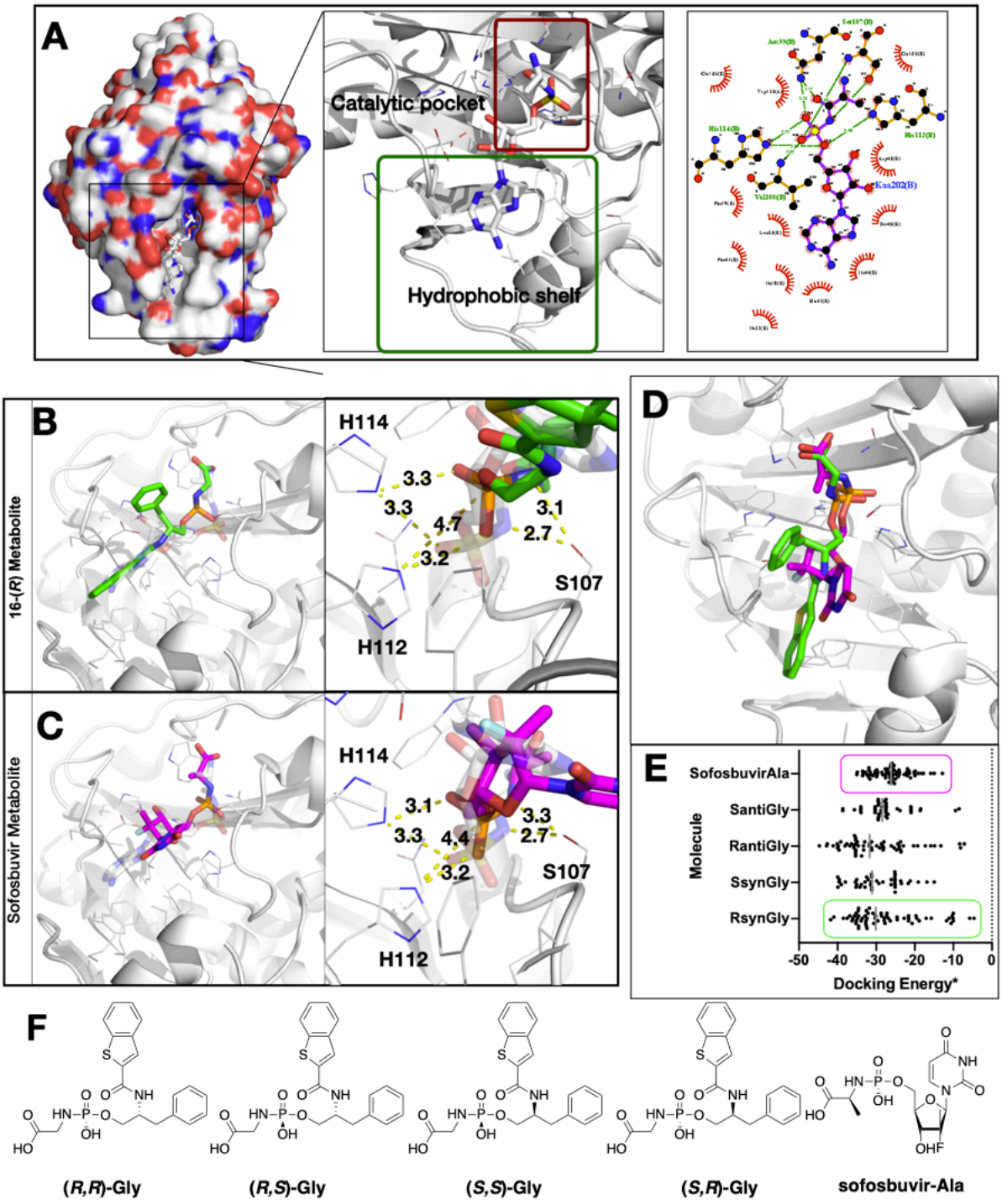

Figure 2.2. Docking studies support the design of high ligand efficiency non-nucleotide Hint1 substrates. A) The Hint1/Lys-AMS cocrystal structure (4EQE) is shown, highlighting that, while the catalytic pocket seems restricted, the pocket containing the distal nucleobase appear more tolerant. B) The best docked pose of the de-esterified metabolite of **16-(*R*)** (**(*R,S*)-Gly)** (solid, green) in the Hint1 catalytic site overlays with the authentic Lys-AMS ligand (transparent, white) [left]. Closer analysis shows the orientation of the docked phosphoramidate in relation to the catalytic residues [right]. C) The docked orientation of the active diastereomer of the

sofosbuvir-Ala metabolite, which is known to be cleaved by Hint (magenta) is overlaid with the co-crystalized Lys-AMS ligand [left] and (*R*)-Gly [right]. D) Summary energy scores for all four possible **16-(*R*)** glycine metabolites in the catalytic site, which were similar to the sofosbuvir-alanine positive control. E) Estimated distances to key catalytic residues (H114, H112, S107) support positioning of the **(*R,S*)-Gly** metabolite in the Hint1 active site. F) Structures and names of all theoretical metabolites used in this docking experiment.

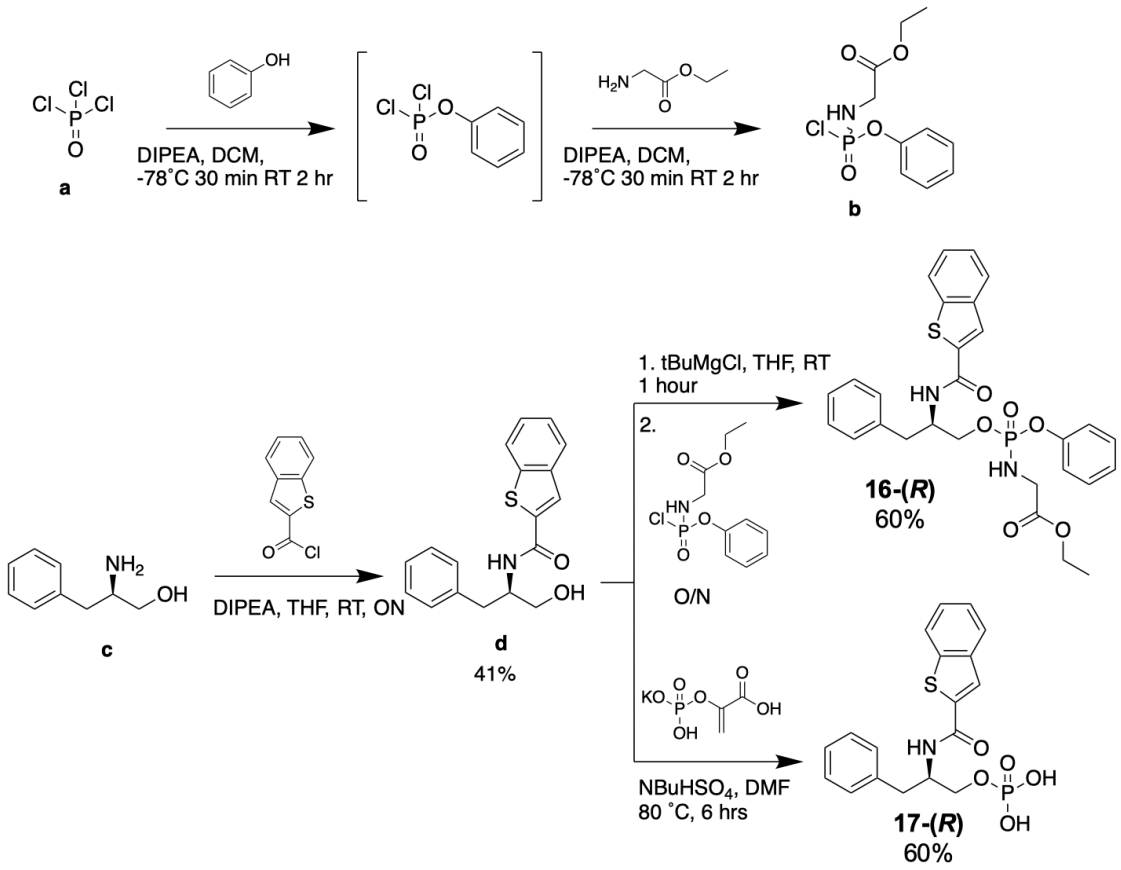

Figure 2.3. Synthesis of phosphoramidates and corresponding phosphate parent molecules for the cellular and *in vitro* inhibition of Pin1. Shown is the synthesis of the *R* enantiomers of **16** and **17**. Synthesis of **16-(*S*)** and **17-(*S*)** were accomplished by identical means. The synthesis of intermediate **b** was completed under argon and drying column. The crude **b** was filtered and carried on into the synthesis of **16**.

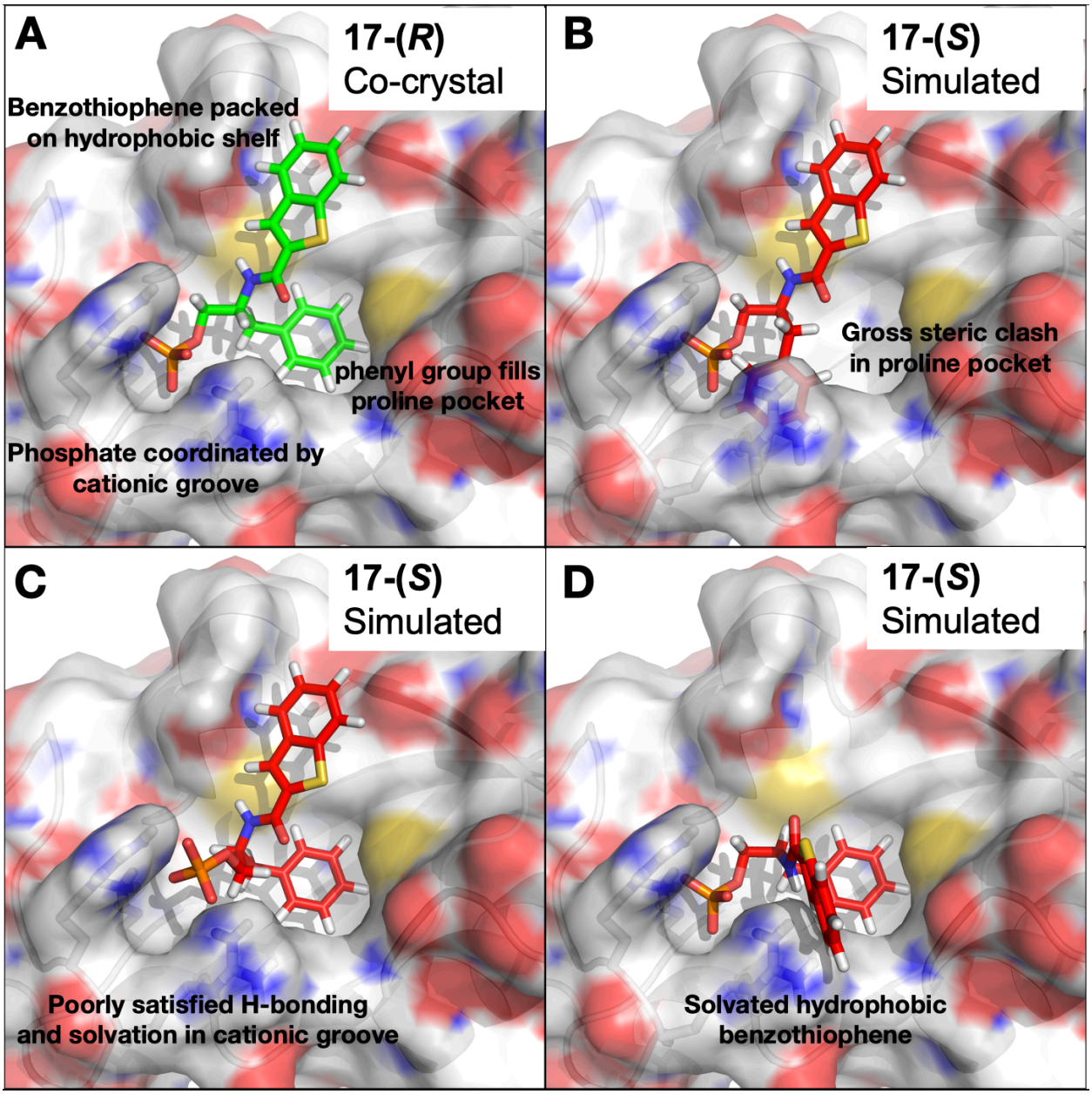

Figure 2.4. *In Sillico* generation of 17-(*S*) poses in the Pin1 catalytic domain support the observation that 17-(*S*) is a significantly weaker binder. A) **17-(*R*)** binds to the Pin1 catalytic domain and adopts a pose that positions the phenyl group in the proline pocket and its benzothiophene on the hydrophobic shelf, setting the phosphate in the cationic groove (K63, R68, and R69). B-D) PDB 3IKD was manipulated in PyMol to invert the stereochemistry of the chiral carbon in **17-(*R*)** to approximate **17-(*S*).** When cationic groove and hydrophobic shelf contacts are maintained (B), the phenyl group sterically clashes with the contour of the proline pocket. If proline pocket and hydrophobic shelf packing are maintained (C), the phosphate is displaced from the cationic groove. If cationic groove and proline pocket are maintained (D), the hydrophobic benzothiophene is left solvated.

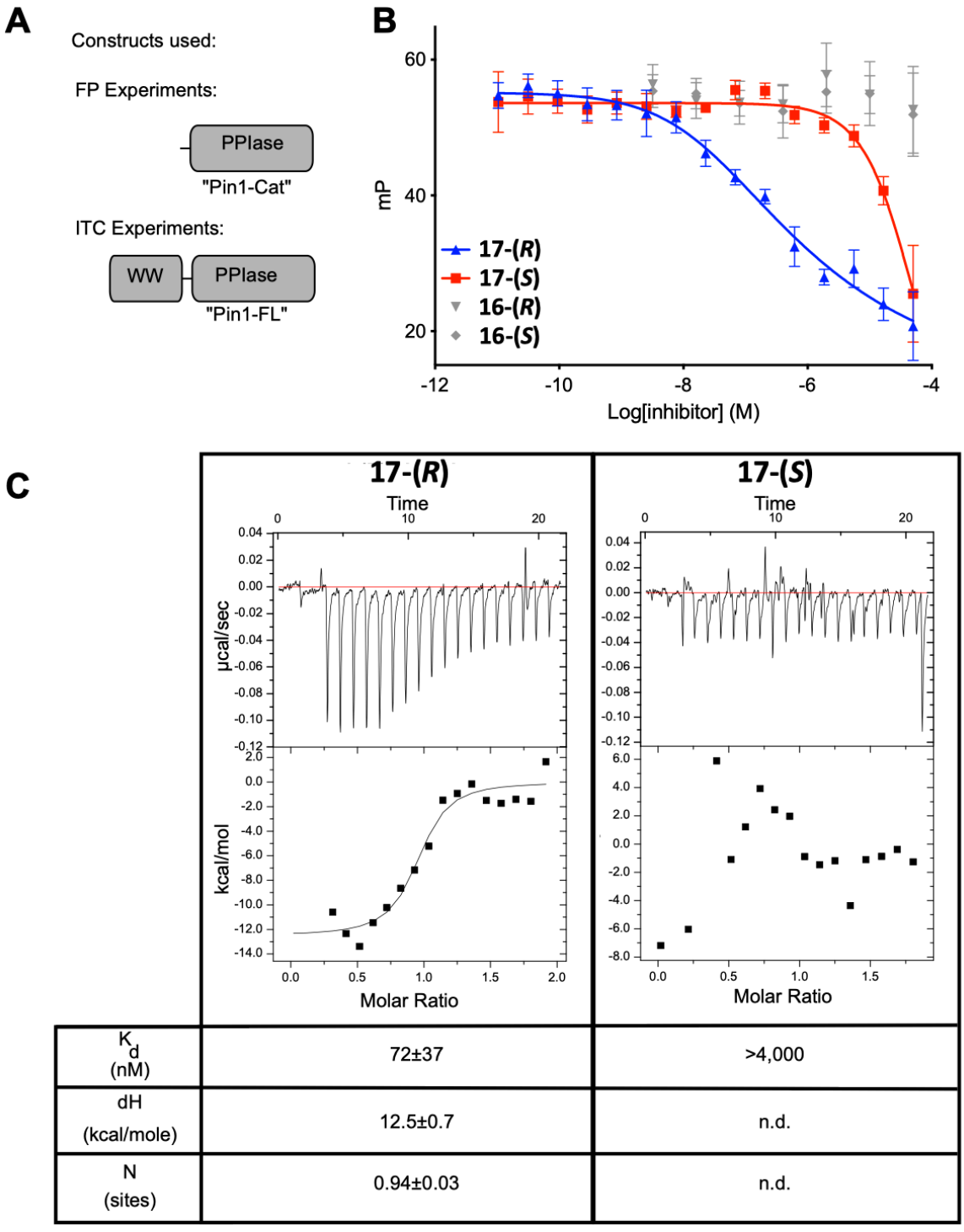

K_d (nM)	72±37	>4,000
dH (kcal/mole)	12.5±0.7	n.d.
N (sites)	0.94±0.03	n.d.

Figure 2.5. *In vitro* Pin1 binding experiments confirm potent monovalent binding of 17-(*R*) and not 17-(*S*). A) Schematic of the constructs used in this study: a truncated Pin1 lacking the WW domain (Pin1-Cat) and full length Pin1 (Pin1-FL). B) **17-(*R*)**, but not **17-(*S*)**, competed with a labelled tracer (FITC-WFYpSPFLE) for binding to Pin1-Cat, as measured by FP. Importantly, neither **17-(*R*)** or **17-(*S*)** bind Pin1. Results are the

average of triplicates and the error bars represent SD. C) ITC experiment confirming that **17-(*R*)** binds Pin1-FL, and with a stoichiometry ~1, consistent with preferential binding to the catalytic domain. Importantly, **17-(*S*)** did not bind detectably.

A

Compound	logP	logPe (cm/sec)
16-(*R*)	0.27	-4.6
17-(*R*)	< -4.6	< -6.3

B

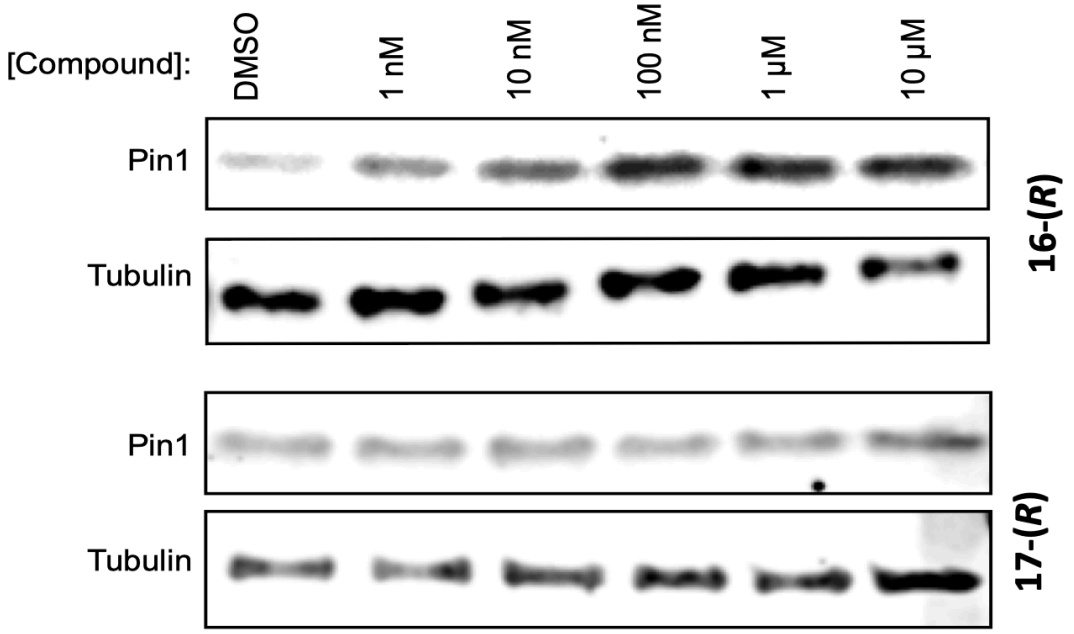

Figure 2.6. *In vitro* physiochemical experiments and differential biomarker response support the membrane permeability of 16 but not 17. A) The experimentally determined lipophilicity and permeability properties support the expected bioavailability improvements of phosphoramidate **17-(*R*)** over the phosphate **16-(*R*)**. Importantly, the measured lipophilicity by octanol/water partitioning and permeability by artificial PAMPA experiments for **16-(*R*)** fall within reasonable correlation with each other when compared to other drug-like molecules which have been measured by these assays.

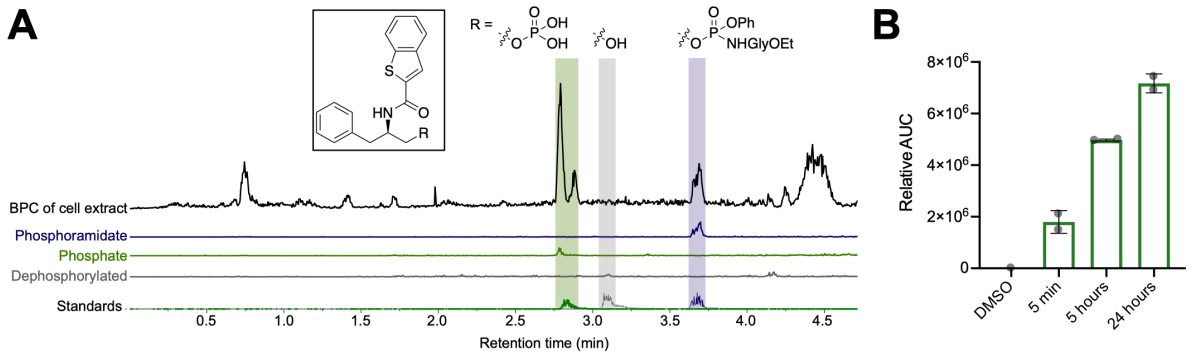

Figure 2.7. Phosphoramidate 16-(*R*) is time-dependently liberated in cells to the parent molecule 17-(*R*). K562 cells treated with **16-(*R*)** were washed, pelleted and extracted with EtOAc. A) The extract was analyzed by UPLC-MS to yield the base peak chromatogram (black). Then, the peaks corresponding to the mass of the phosphoramidate (purple), phosphate (green) and the dephosphorylated metabolite (gray) were identified in the treated sample and compared to the approximate elution window of the authentic standards (bottom). B) To understand release of the phosphate product over time, a time course experiment was conducted and the peak area quantified. A solvent control (DMSO) was used to subtract the background. The average of duplicate experiments is shown, with the full range denoted with bars.

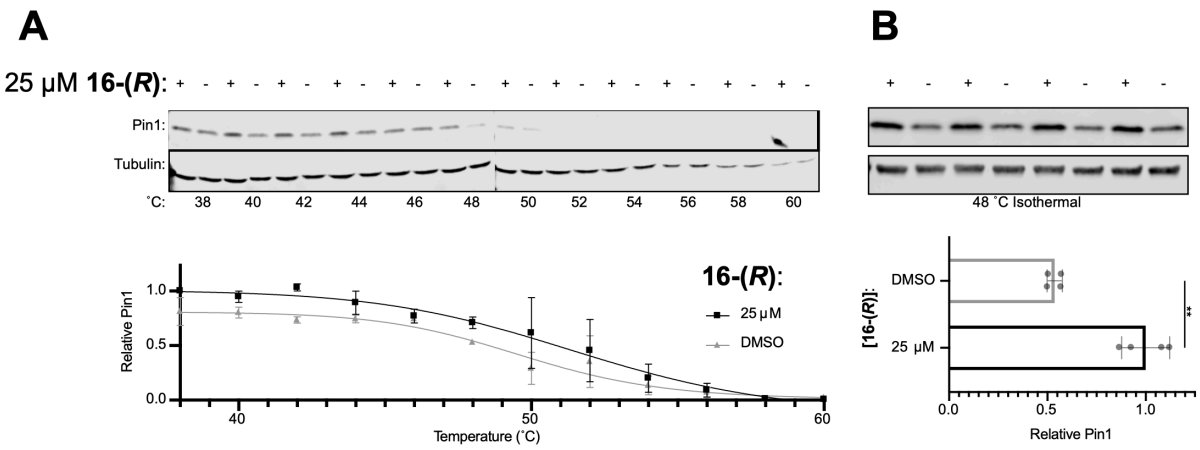

Figure 2.8. Validation of target engagement in cells by CETSA. A) K562 cells were treated with **16-(*R*)**, heated at temperatures between 38 to 60 ˚C, and the soluble fraction assayed for Pin1 abundance by western blot. Treatment with **16-(*R*)** led to stabilization of Pin1, compared to the mock treated (quantified below). Interestingly, **16-(*S*)** also resulted in an increased solubility of Pin1 in this assay. We expect that this was due to an intermediate folding state of Pin1 being capable of accommodating the *S* enantiomer resulting in a pharmacological chaperone activity (data not shown). Results are the average of three independent experiments and error bars represent SEM. B) Similar results were observed in MDA-MB-231 cells, treated at a fixed temperature (48 ˚C) in biological quadruplicates (quantified below). ** p value < 0.01

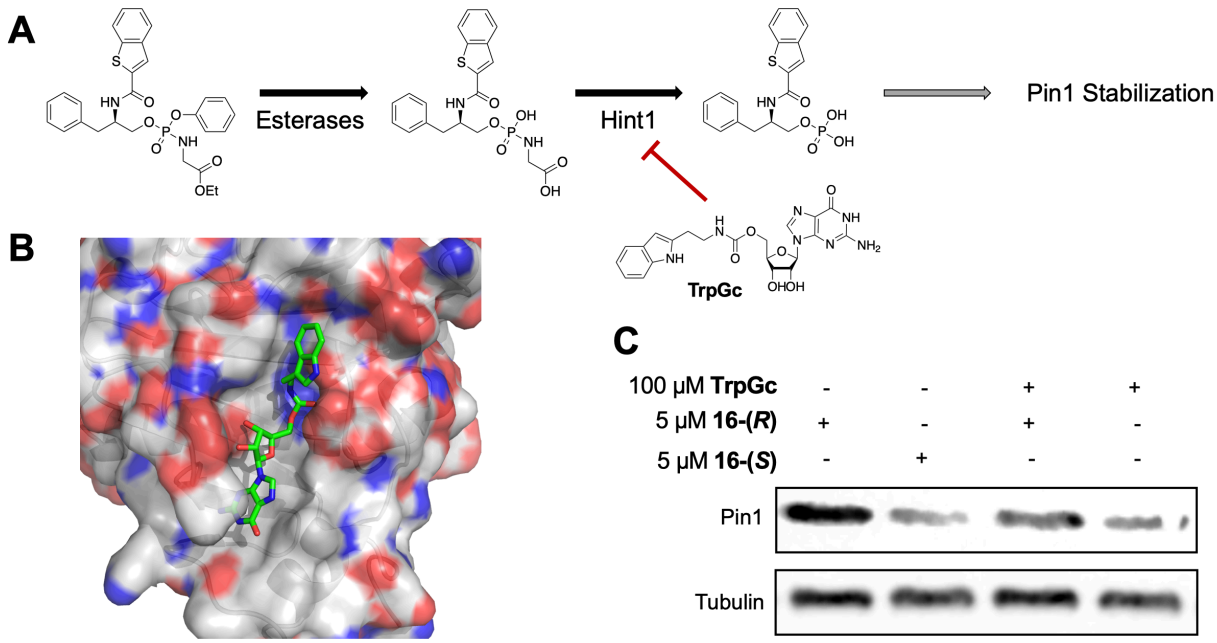

Figure 2.9. Chemical inhibition of Hint1 suppresses activity of 16-(*R*) supporting a Hint1-dependent liberation mechanism. A) Proposed liberation scheme of **16-(*R*)** with **TrpGc**, a previously described Hint1 inhibitor and primary biomarker for target engagement, Pin1 stabilization, denoted with a gray arrow. It is expected that if Hint1 is responsible for liberation of the parent **17-(*R*)**, then biomarker response would be diminished by **TrpGc 16-(*R*)** combination treatment. B) Co-crystal structure of TrpGc bound to Hint1 (accession: 5I2E, (34)). C) Hint1 inhibition with TrpGc reduces the stabilization of Pin1 by **16-(*R*)**. Importantly, **16-(*S*)** does not induce stabilization of Pin1 under normal growth conditions, supporting the hypothesis that **16-(*S*)** does not interact with folded Pin1 in cells.

CHAPTER 3

BIOLOGICAL EVALUATION OF POTENT PIN1 INHIBITORS IN CANCER CELLS

Daniel MC Schwarz, Matthew Callahan, Jason E Gestwicki

Background. The enrichment of proline-directed phosphorylations in processes such as cell-cycle progression, apoptosis, and differentiation has inspired decades of research into Pin1's role in cancer (1,2). To date, Pin1-dependent isomerization events have been proposed in dozens of oncoproteins and tumor suppressors, including some of the most sought-after targets in oncology (i.e. c-Myc, N-Myc, p53, c-Jun, and many cyclins) (Reviewed in 3). Throughout this process, research has been limited to genetic perturbation (often knockdown (KD) or knockout (KO) experiments), crude chemical tools with poor/unknown selectivity, and *in vitro* reconstituted systems. While these efforts have been quite useful for identifying putative Pin1 substrates and Pin1-dependent biology, there is a pressing need for potent and selective chemical probes for Pin1. Such molecules would resolve key questions in the field. For example, Pin1 contains two domains which bind to identical motifs (4). In other systems, such as epigenetic enzymes, chemical probes that bind only one of the domains have played a critical role in revealing how these enzymes work . While it's been implied in the literature that Pin1 catalytic activity is what drives its functions, recently developed, competitive inhibitors for Pin1 have surprisingly modest effects, which are less than what would be expected from knockdown (5–7). These results suggest that the non-catalytic functions of Pin1 (i.e. scaffolding by the WW domain) may be playing an important role in its biology. The observation that **17-(*R*)** only binds the catalytic domain in the context of full-length wildtype Pin1. This finding suggests that **18-(*R*)** can be used to, for first time in intact biological systems, differentiate which Pin1 roles are attributed to the catalytic function and which ones might be independent.

As discussed in Chapter 1, the availability of **18-(*R*)** provides an additional layer of temporal control that seems critical in probing Pin1 biology. It has been especially difficult to study Pin1 biology using genetics because the enzyme is involved in dynamic biological processes. The rate of peptidyl-prolyl isomerization in the absence of a PPIase is slow;

however, the isomerization does happen intrinsically (8). Thus, it seems important to use chemical probes that acutely disrupt its function. Furthermore, reversible inhibition is extremely valuable for this level of temporal tunability, as it allows washout and a return to homeostasis.

Reversible Active Site Pin1 Inhibition in Intact Cellular Systems. PC3 cells have been useful models for studying Pin1 biology (9). These cells harbor a PTEN deletion and therefore have aberrant PI3K/AKT signaling independent of growth factor (10). They have been demonstrated to be dependent on Pin1 for growth in low-serum or in low-confluence growth contexts. Early on, most experiments which determined the dependence of cancers on Pin1 were done with WW-domain dominant negative mutation or knockdown of PIN1 by RNAi (9,11). Since these approaches fail to validate the importance of Pin1 catalytic function in this phenotype, we repeated these experiments with **18-(*R*)** or the control molecule **18-(*S*)**. Interestingly, these phenotypes are recapitulated by Pin1 active site inhibition suggesting a catalytic role for Pin1 in this process (Figure 3.1A). To further evaluate the role of Pin1 catalysis in PI3K/AKT signaling, a kinetic experiment looking at 4E-BP1 phosphorylation in response to pathway activation was conducted. While the impact of Pin1 KD on AKT activation has been evaluated (12), the effect on downstream phosphorylations had not. In this experiment, the inhibition of Pin1 with **18-(*R*)** but not treatment with the control molecule **18-(*S*)** resulted in the slowing of 4E-BP1 phosphorylation in response to EGF stimulation (Figure 3.1B).

One challenge of Pin1 biology is the subtle physical impact of substrate catalysis. In order to detect a Pin1 isomerization event in cells, such great lengths have been taken as to develop conformationally-specific antibodies for *cis*- vs *trans*-peptidyl-prolyl bonds (13). Importantly, even the accuracy of these antibodies for one conformer over another have

been contested. Interestingly, a common mechanism of Pin1 function is to sterically occlude or expose a phosphorylation to a phosphatase. This inspired the use of an *in vitro* dephosphorylation stability assay to test whether Pin1 inhibition resulted in a distinct conformational bias in a given substrate or putative substrate. While this approach does not resolve the precise conformation, it does have the potential to provide comparative information between proteins which exist in the presence or absence of Pin1 catalysis. Interestingly, with a bone fide Pin1 substrate (RNA Pol II pSer 5), Pin1 inhibition with **16-(*R*)** but not control compound treatment reduced the stability to *in vitro* dephosphorylation with lambda-phosphatase (Figure 3.2).

One remaining question remaining about the effect of Pin1 inhibition 4E-BP1 phosphorylation was whether the effect was direct or upstream of the assayed phosphorylation. To address this, the partial dephosphorylation assay was repeated on Pin1-treated PC3 lysate. If Pin1 inhibition impacts the stability of 4E-BP1 phosphorylation in this assay, this supports the idea that the phospho-protein is in a different conformation to the untreated likely due to the lack of Pin1-dependent isomerization of proline-directed phosphorylations. In testing the potential Pin1 substrate 4E-BP1 which is more slowly phosphorylated in the presence of Pin1 inhibitor, A similar compound-specific reduction in stability was detected as compared to the Ser5 phosphorylation on RNA polymerase II (Figure 3.2).

Interestingly, there are some divergent phenotypes between genetic perturbation and inhibition as well. For instance, while the knockdown or knockout of Pin1, even over long timeframes, is insufficient to inhibit cell growth in all cancers tested in DepMap (14) (Broad Institute), chemical inhibition of Pin1 is frequently inhibitory of colony formation and is even capable of inhibiting growth in certain cell lines in short-term 2D growth experiments. For

instance, when submitted to the NCI-60 panel (15), **18-(*R*)** more potently inhibited the growth of many cell lines as compared to **18-(*S*)** (Figure 3.3). Interestingly, MDA-MB-468 cells were inhibited quite potently and specifically, consistent with cell-type sensitivity of covalent selective tool molecule **12** (6). Further, all but one cell line (A498) which showed significant anti-proliferative effect were specific for **18-(*R*)** as compared to **18-(*S*)**. Together, these data suggest that Pin1 inhibition is responsible for the effect.

Finally, the impact of Pin1 inhibition on the proteome was explored in PC3 cells by a label-free quantitation mass spectrometry experiment (Figure 3.4). PC3 cells were treated with either **18-(*R*) or 18-(*S*)** under normal 2D growth conditions. Total cell lysate was subject to tryptic digest and LC-MS/MS analysis. High-level analysis of changes in protein abundance under treatment with **18-(*R*)** as compared to **18-(*S*)** show a handful of proteins mildly perturbed in concentration. Unfortunately, since this shotgun experiment did not enrich for phospho-peptides, there is extremely limited data in the dataset on the impact on the phospho-proteome; however, some biologies are enriched in the up/down-regulated proteins by gene ontology (GO) analysis using String Database (16). For instance, RNA processing proteins were enriched in the hits with ≥1.5-fold change and p-value ≤ 0.05. Considering the mild effect on protein abundance, future experiments are necessary to optimize the experimental design for the detection and and validation of the effects of perturbation. For instance, higher concentrations of inhibitor and control molecule may be used and/or longer timescales of treatment – each of these may boost the impact on changes in protein abundance.

Broad Kinase Synergy Observed with Pin1 Inhibition. Pin1 is a key chaperone of proline-directed phosphorylations. It therefore follows that Pin1 inhibition would broadly dysregulate phosphorylative signaling as proline-directed phosphorylations are enriched

at the most downstream signaling steps (i.e. transcription regulation). While a discreet observation of functional interactions between Pin1 and CDK2 has reported (17), no unbiased evaluation of Pin1-kinase functional interaction has been described in the literature.

To test the scope of Pin1-kinase interaction, identical viability screens were conducted for four cell lines: K562, PC3, and MDA-MB-231. These cell lines are well studied and characterized and represent a range of oncogenic pathologies. To determine if Pin1 inhibition potentiated the activity of kinase inhibitors in each cell line, 380 kinase inhibitors from the Selleckchem kinase inhibitor library were individually dosed on cells at 1 μM with or without 250 nM **18-(*R*)** in duplicate. The cells were grown for 72 hours and viability was determined by ATPglo assay. Percent change in viability was determined for each kinase inhibitor in combination with **18-(*R*)** (Figure 3.6A).

Interestingly, each cell type had some overlapping and some distinct hits (Figure 3.6B-D). Enriched hits tended to be indicative of the drivers of cell growth in the individual cell line. For instance, in Philadelphia chromosome positive K562 cells (18) BCR-Abl and promiscuous tyrosine kinase inhibitors were enriched. Similarly, in PC3 cells which harbor a PTEN deletion (10) and consequently have aberrantly active PI3K/AKT signaling, were enriched for PI3K, AKT, and mTOR inhibitor potentiation. Strikingly, the only cell line which enriched for CDK inhibitors (one of the more well-represented proline-directed kinase inhibitor classes in this library) was MDA-MB-231. This cell line relies on heavily on Myc which has been shown to be sensitive to pan-CDK inhibition (19).

To interrogate the potentiation of CDK inhibitors more mechanistically, Pin1 inhibition in combination with the specific CDK4/6 inhibitor and clinically approved drug palbociclib was

evaluated in MCF7 cells. While this is admittedly a distinct system from where the Pin1-CDK potentiation was observed, the mechanism of how palbociclib (a highly selective CDK4/6 inhibitor (20)) inhibits the growth of Her2-/ER+ breast cancer (of which MCF7 cells are approximately representative (21)) is well defined in the literature. Indeed, many of the pre-clinical experiments to evaluate the effect of palbociclib were conducted in MCF7 cells. This mechanistic clarity and precedent are essential for the efficient evaluation of Pin1-CDK cooperation.

Briefly, the complex of CDK4/6 and cyclin D1 is catalytically active and initiates the phosphorylation and partial inactivation of the tumor suppressor retinoblastoma protein (Rb). The hypo-phosphorylated species of Rb is theorized to allow low level activity of the E2F (also known as c-Jun) transcription factor sufficient for the expression of cyclin E1 which binds and activates CDK2. This CDK2-Cyclin E1 complex further phosphorylates and fully inhibits the Rb-mediated inhibition of E2F transcription (22). Interestingly, the aberrant overexpression of cyclin E1 is commonly seen in patients who have evolved resistance to palbociclib. The prevailing mechanistic theory behind this resistance is the CDK2-cylin E1 fully phosphorylates Rb and consequently fully activates E2F transcription regardless of CDK4/6-cyclin D1 levels or activity (23).

Importantly, there is mild potentiation of the activity of palbociclib in MCF7. Interestingly, HCT116 cells which aberrantly express cyclin E1 (24) – recapitulating the aforementioned clinical palbociclib resistance mechanism – also are made sensitive to palbociclib treatment upon Pin1 inhibition. Following these exciting observations, clarification of the mechanism of potentiation was necessary.

It's known that palbociclib treatment induces cyclin D1 expression over 24 hours of treatment (25). It's also been reported in the literature that Pin1 depletion by KO and KD destabilizes cyclin D1 (26). It may follow that Pin1 inhibition will sensitize MCF7 cells to palbociclib treatment by reducing the effective concentration of the target (i.e. the catalytically active CDK4/6-cyclin D1 complex). Indeed, Pin1 inhibition in combination with palbociclib does reduce the rate of cyclin D1 induction and significantly reduce the half-life – it follows that this would therefore reduce the half-life of the active complex.

HCT116 cells express high levels of cyclin E1 and are consequently resistant to palbociclib treatment. Pin1 is known to be required for the transcriptional regulation of the E2F and Myc transcription factors which are responsible for the expression of cyclin E1. Consistent with this, Pin1 inhibition in HCT116 cells reduces cyclin E1 levels significantly. Interestingly, this is not through the reduction in cyclin E1 half-life as is seen with MCF7 cells. One potential explanation for this disconnect is transcriptional regulation of cyclin E1 expression. Indeed, Pin1 is proposed to regulate E2F any Myc transcription factors which are involved in the expression of cyclin E1 (27,28). Interesting there was no detectable potentiation of the functional readout of CDK4/6 inhibition (i.e. Rb phosphorylation). Surprisingly, it appears that the combination of **18-(*R*)** and palbociclib led to a marked reduction in Rb concentration, which is expected to activate cell-cycle progression (29). These results suggest an alternative mechanism of cooperativity between Pin1 and CDK4/6 inhibition than the one proposed and warrant further examination.

Tools, Strategies, and Future Directions. Herein was discussed the conception, design, and evaluation of an unprecedentedly potent inhibitor of the peptidyl-prolyl isomerase Pin1. While these studies are compelling evidence of a novel approach to delivering non-nucleotide phosphate prodrugs into the cell and a demonstration of best-in-class inhibition

of Pin1 many questions remain. Specifically, the biophysical effects of the molecule on Pin1 structure, the functional specificity of the various metabolites in cells, the value of the molecules for use *in vivo*, and finally the impact of Pin1 catalytic inhibition on the homeostasis of the phospho-proteome.

On the topic of specificity, while we can reasonably expect that these molecules are somewhat specific and that the results we see here are representative of Pin1 inhibition (due to the use of an inactive enantiomer control), the absolute specificity of the prodrug and parent are unknown. Some effort has been put into developing a broader candidate-based CETSA experiment to interrogate this; however, no conclusive data has been generated. CETSA is a laborious and low-throughput assay when conducted by western blot. Indeed, most CETSA done at scale is done using an AlphaLisa readout. This approach would likely be required for practically optimizing conditions for multiple candidate targets.

Additionally, while these molecules are exceptionally effective in cells, the evaluation of their usefulness *in vivo* has yet to be shown. This specific approach to prodrugging phosphates has some limitations in wildtype mice – the uniquely high esterase activity in mouse plasma begins uncaging the phosphate before diffusion across the cell membrane may occur. Indeed, to use ProTides or other similar phosphoramidates in mice, esterase KO mice or chemical stabilizers must be used. In the future, it would be great to design next-generation phosphoramidates which utilize the anchimerically activated approach recently published for use with nucleotides. In this approach, an oxygen-linked alkyl thioether and a nitrogen-linked tryptamine are used to produce a phosphoramidate which first undergoes a slow chemical liberation of the thioether and subsequent Hint1-mediated

hydrolysis of the phosphoramide bond. Since these molecules remove the requirement for esterase activity, these molecules may be used in wildtype mice.

Finally, further analysis of the general effects of Pin1 inhibition on cancer cells is needed. For example, no evaluation of the broad impact of Pin1 inhibition on the phospho-proteome has been published. Given the recent availability of high-quality tool molecules, these experiments could be repeated with multiple approaches to start to parse the difference between inhibition of enzymatic activity only, competitive inhibition of both catalytic and WW-domain-mediated substrate binding, and degradation of the entire Pin1 molecules. Specifically, experiments which evaluate the steady-state impact of Pin1 inhibition on the phospho-proteome. as well as exploring the *in vitro* phosphatase stability of the proteome following Pin1 inhibition. Between these experiments, greater understanding of Pin1-dependent signaling and direct Pin1 substrates could be achieved, respectively.

Materials and Methods:

Colony Formation Assay: PC3 cells were plated on poly-d-lysine-coated 12-well plates (250 cells per well) with the indicated compound treatment. Cells were allowed to proliferate until untreated wells reached colonies of > 50 cells each (~2.5 weeks). Media was removed, cells were stained with Crystal Violet stain (30), and plate was imaged using a document scanner. Colonies were manually counted.

EGF Stimulation of 4E-BP1 Phosphorylation: PC3 cells were plated in a 12-well plate at 50% confluency. The cells were grown in the absence of serum for 24 hours under otherwise normal growth conditions. At the desired timepoints, cells were stimulated with

EGF at 100 nM concentration. Cells were returned to normal growth conditions until harvesting. To harvest, cells were washed with cold PBS and plunged into liquid nitrogen. Cells were lysed by boiling in 4% SDS in TBS with 1 mM DTT.

Partial Dephosphorylation: Cells were treated with the desired compound for 24 hours and lysed by repeated freezing and thawing in PBS with PMSF. Following clarification by centrifugation, supernatant was combined 1:1 by volume with lambda phosphatase (New England Bioscience) and incubated for the desired time at 37˚C. To quench the reaction, 3x loading buffer was added to the reaction.

NCI-60 Cell Panel: 18-(*R*) and **18-(*S*)** were submitted to the NCI-60 cell panel at the Developmental Therapeutics Program of the National Cancer Institute.

Treatment and Lysis for LFQ Proteomics Experiment: PC3 cells were plated in T75 flasks and grown to 50% confluency. At this time, media was swapped for media containing 250 nM **18-(*R*)** or **18-(*S*)**. After 24 hours of treatment, cells were lysed in 4% SDS in TBS with 1 mM DTT.

Peptide Preparation for LFQ Proteomics Experiment: Peptides were prepared by Filter Aided Sample Preparation (FASP) as previously described. Briefly, lysate was denatured further in 8M urea bound to a nitrocellulose spin filter, alkylated with iodoacetamide, and trypsinized. The peptides were subsequently eluted and desalted with a C18 column. Peptides were analyzed on a Thermo Fisher Lumos LC-MS/MS.

Kinase Synergy Screens: The desired cell line was plated at 5,000 cells per well in a 384-well white-walled plate and treated with 1 μM of each of the 380 kinase inhibitors in

the Selleck Chem Kinase Inhibitor Library (Cat# 1200) in DMEM complete or RPMI complete. After 72 hours of growth, 50 µL of Cell Titer Glo reagent (Promega) was added and incubated on a rotary shaker for 10 min. Luminescence was recorded on a Spectromax M5 plate reader (Molecular Devices).

18-(*R*)/Palbociclib Combination Evaluation (Steady-State): The desired molecule or combination of inhibitors was diluted to 1 µM in DMEM complete and 200,000 cells/mL were suspended in the resultant solution. 1 mL of the suspension was plated in a 12-well plate and cells were grown under normal growth conditions for 72 hours. Cells were lysed with 4% SDS in TBS with 1 mM DTT and the clarified lysate was analyzed by western blot.

CHX-Chase Experiments: Cells were treated as above for 24 hours with the desired compound or combination of compounds. Following the 24 hour treatment a solution, CHX was added at the desired timepoint (in the presence of sustained inhibitor or inhibitor combination treatment. Cells were subsequently lysed with 4% SDS in TBS with 1 mM DTT and the clarified lysate was analyzed by western blot.

18-(*R*)/Palbociclib Combination Evaluation (Kinetic): Cells were plated at the density of 200,000 cells/well in DMEM complete and grown under normal growth conditions. At the desired timepoint, the desired inhibitor or inhibitor combination was added to the cells. Cells were lysed with 4% SDS in TBS with 1 mM DTT and the clarified lysate was analyzed by western blot.

MTT viability assay: PC3 cells were plated in a poly-d-lysine-coated clear 96-well plate at 5,000 cells/well and treated with 1µM **18-(*R*)**, **18-(*S*)**, or a matched concentration of

DMSO. Cells were allowed to proliferate for 72 hours in their given conditions. Following the out-growth, media was replaced with 50 µL untreated serum free media supplemented with 1 mg/mL MTT reagent and cells were incubated in normal growth conditions for three hours. An additional row of the plate which lacked cells was treated with MTT-media as a negative control. Media was then aspirated carefully and replaced with 50 µL DMSO and nutated for 10 minutes. Plate was analyzed by measuring A_{590} on a Spectromax M5 plate reader (Molecular Devices). Viability was determined by the following equation:

$$\frac{(A_{590,treated} - blank)}{(A_{590,untreated} - blank)} = relative\ viability$$

References:

1. Lu KP, Liou Y, Zhou XZ, Liou Y. Pinning down phosphorylation signaling. Trends Cell Biol [Internet]. 2002;12(4):164–72. Available from: http://dx.doi.org/10.1016/S0962-8924(02)02253-5
2. Hall FL, Vulliet PR. Proline-directed protein phosphorylation and cell cycle regulation. Curr Opin Cell Biol. 1991;3(2):176–84.
3. Zhou XZ, Lu KP. The isomerase Pin1 controls numerous cancer-driving pathways acting as a unique drug target. Nat Rev Cancer. 2016;16(7):463–78.
4. Momin M, Yao XQ, Thor W, Hamelberg D. Substrate Sequence Determines Catalytic Activities, Domain-Binding Preferences, and Allosteric Mechanisms in Pin1. J Phys Chem B. 2018;122(25):6521–7.
5. Pinch BJ, Doctor ZM, Nabet B, Browne CM, Seo HS, Mohardt ML, et al. Identification of a potent and selective covalent Pin1 inhibitor. Nat Chem Biol [Internet]. 2020; Available from: http://dx.doi.org/10.1038/s41589-020-0550-9
6. Dubiella C, Pinch BJ, Koikawa K, Zaidman D, Poon E, Manz TD, et al. Sulfopin is a covalent inhibitor of Pin1 that blocks Myc-driven tumors in vivo. Nat Chem Biol [Internet]. 2021; Available from: http://www.ncbi.nlm.nih.gov/pubmed/33972797
7. Schwarz DMC, Williams SK, Dillenburg M, Wagner CR, Gestwicki JE. A Phosphoramidate Strategy Enables Membrane Permeability of a Non-nucleotide Inhibitor of the Prolyl Isomerase Pin1. ACS Med Chem Lett. 2020;11(9):1704–10.
8. Garel JR, Baldwin RL. Both the fast and slow refolding reactions of Ribonuclease A yield native enzyme. Proc Natl Acad Sci U S A. 1973;70(12 (I)):3347–51.
9. Ryo A, Uemura H, Ishiguro H, Saitoh T, Yamaguchi A, Perrem K, et al. Stable suppression of tumorigenicity by Pin1-targeted RNA interference in prostate cancer. Clin Cancer Res. 2005;11(20):7523–31.
10. Wee S, Wiederschain D, Maira SM, Loo A, Miller C, DeBeaumont R, et al. PTEN-

deficient cancers depend on PIK3CB. Proc Natl Acad Sci U S A. 2008;105(35):13057–62.

11. Ryo A, Liou Y, Wulf G, Nakamura M, Lee SW, Lu KP. PIN1 Is an E2F Target Gene Essential for Neu / Ras -Induced Transformation of Mammary Epithelial Cells. 2002;22(15):5281–95.
12. Zhang Z, Yu W, Zheng M, Liao X, Wang J, Yang D, et al. Pin1 inhibition potently suppresses gastric cancer growth and blocks PI3K/AKT and Wnt/β-catenin oncogenic pathways. Mol Carcinog. 2019;58(8):1450–64.
13. Nakamura K, Greenwood A, Binder L, Bigio EH, Denial S, Nicholson L, et al. Proline isomer-specific antibodies reveal the early pathogenic tau conformation in Alzheimer's disease. Cell [Internet]. 2012;149(1):232–44. Available from: http://dx.doi.org/10.1016/j.cell.2012.02.016
14. Tsherniak A, Vazquez F, Montgomery PG, Weir BA, Kryukov G, Cowley GS, et al. Defining a Cancer Dependency Map. Cell [Internet]. 2017;170(3):564-576.e16. Available from: http://dx.doi.org/10.1016/j.cell.2017.06.010
15. Alley MC, Scudiero DA, Monks A, Hursey M, Czerwinski MJ, Fine DL, et al. Feasibility of Drug Screening with Panels of Human Tumor Cell Lines Using a Microculture Tetrazolium Assay. Cancer Res. 1988;48(3):584–8.
16. Szklarczyk D, Gable AL, Lyon D, Junge A, Wyder S, Huerta-Cepas J, et al. STRING v11: Protein-protein association networks with increased coverage, supporting functional discovery in genome-wide experimental datasets. Nucleic Acids Res. 2019;47(D1):D607–13.
17. Cheng CW, Leong KW, Ng YM, Kwong YL, Tse E. The peptidyl-prolyl isomerase PIN1 relieves cyclin-dependent kinase 2 (CDK2) inhibition by the CDK inhibitor p27. J Biol Chem [Internet]. 2017;292(52):21431–41. Available from: http://dx.doi.org/10.1074/jbc.M117.801373
18. Lozzio BB, Lozzio CB. Properties of the K562 cell line derived from a patient with chronic

myeloid leukemia. Int J Cancer. 1977;19(1):136.

19. Lawson DA, Bhakta NR, Kessenbrock K, Prummel KD, Yu Y, Takai K, et al. Single-cell analysis reveals a stem-cell program in human metastatic breast cancer cells. Nature. 2015;526(7571):131–5.

20. Fry DW, Harvey PJ, Keller PR, Elliott WL, Meade MA, Trachet E, et al. Specific inhibition of cyclin-dependent kinase 4/6 by PD 0332991 and associated antitumor activity in human tumor xenografts. Mol Cancer Ther. 2004;3(11):1427–37.

21. Comşa Ş, Cîmpean AM, Raica M. The story of MCF-7 breast cancer cell line: 40 Years of experience in research. Anticancer Res. 2015;35(6):3147–54.

22. Satyanarayana A, Kaldis P. Mammalian cell-cycle regulation: Several cdks, numerous cyclins and diverse compensatory mechanisms. Oncogene. 2009;28(33):2925–39.

23. Li Z, Zou W, Zhang J, Zhang Y, Xu Q, Li S, et al. Mechanisms of CDK4/6 Inhibitor Resistance in Luminal Breast Cancer. Front Pharmacol. 2020;11(November):1–10.

24. Lu K, Shih C, Teicher BA. Expression of pRB, cyclin/cyclin-dependent kinases and E2F1/DP-1 in human tumor lines in cell culture and in xenograft tissues and response to cell cycle agents. Cancer Chemother Pharmacol. 2000;46(4):293–304.

25. Yang C, Li Z, Bhatt T, Dickler M, Giri D, Scaltriti M, et al. Acquired CDK6 amplification promotes breast cancer resistance to CDK4/6 inhibitors and loss of ER signaling and dependence. Oncogene. 2017;36(16):2255–64.

26. Fujimori F, Takahashi K, Uchida C, Uchida T. Mice Lacking Pin1 Develop Normally , but Are Defective in Entering Cell Cycle from G 0 Arrest. 1999;663:658–63.

27. Ligase U, Csizmok V, Montecchio M, Lin H, Tyers M, Sunnerhagen M, et al. Multivalent Interactions with Fbw7 and Pin1 Facilitate Recognition of c-Jun by the SCF Fbw7 Article Multivalent Interactions with Fbw7 and Pin1 Facilitate Recognition of c-Jun by the SCF Fbw7 Ubiquitin Ligase. Struct Des [Internet]. 2018;1–12. Available from: https://doi.org/10.1016/j.str.2017.11.003

28. Wulf GM, Ryo A, Wulf GG, Lee SW, Niu T, Lu KP. Pin1 is overexpressed in breast cancer and potentiates the transcriptional activity of phosphorylated c-Jun towards the cyclin D1 gene. Embo J. 2001;20(13):3459–72.

29. Knudsen ES, Kathleen McClendon A, Franco J, Ertel A, Fortina P, Witkiewicz AK. RB loss contributes to aggressive tumor phenotypes in MYC-driven triple negative breast cancer. Cell Cycle. 2015;14(1):109–22.

30. Crystal Violet Staining Solution (0.5%). Cold Spring Harb Protoc. 2016;

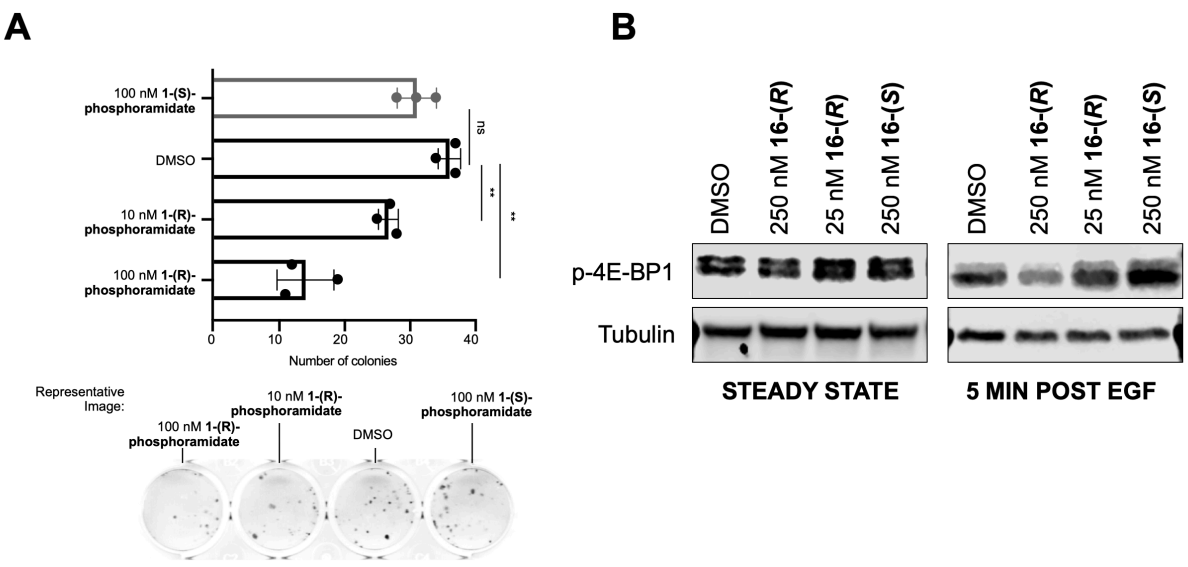

Figure 3.1. Recapitulation and expansion of Pin1 loss phenotypes in neuroendocrine prostate cancer cell line PC3. A) Reproduction of one of the earliest antiproliferative activities of Pin1 perturbation was seen with **16-(*R*)** but not **16-(*S*)**. B) Pin1 inhibition had no effect on steady-state levels of 4E-BP1 phosphorylation by mTORC1 (4E-BP1 pThr37,46) in the presence (shown) or absence (data not shown) of serum. Interestingly, the impact of Pin1 inhibition was profound when assayed 5 minutes following EGF stimulation.

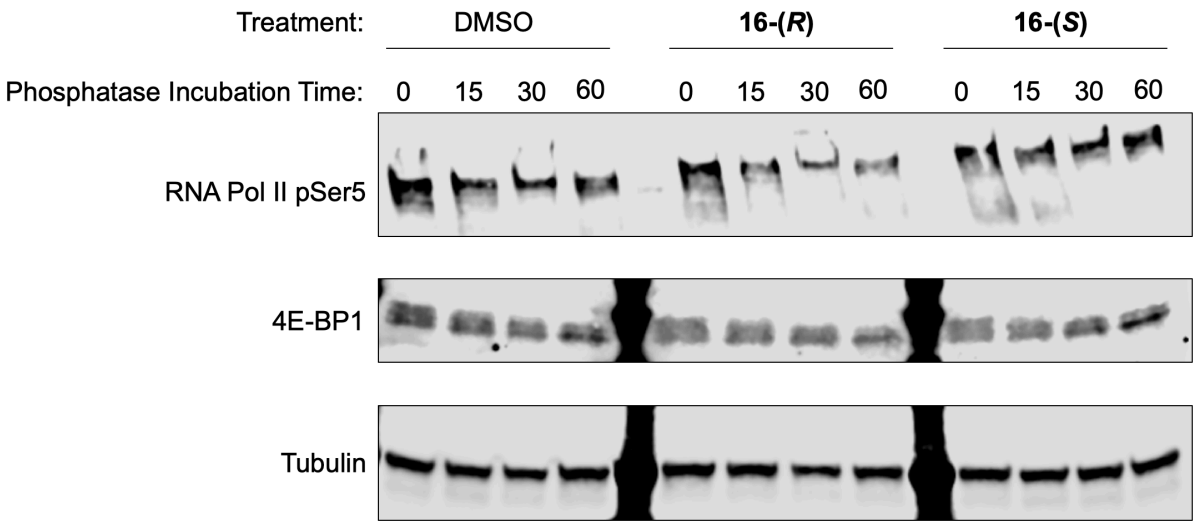

Figure 3.2. Partial de-phosphorylation as a method of validating Pin1 substrates. In an effort toward developing a method to identify Pin1 substrates, a partial dephosphorylation assay was designed. In incubating DMSO, **16-(*R*)**, or **16-(*S*)** treated lysate with lambda-phosphatase, destabilization of the known Pin1 substrate pSer5 of RNA Pol II was observed. Following on the observation that Pin1 inhibition was effective at slowing the phosphorylation of 4E-BP1, a total 4E-BP1 antibody was used to probe phosphorylation status of the protein by gel shift. Excitingly, it appears that Pin1 inhibition also sensitizes 4E-BP1 to lambda phosphatase dephosphorylation *in vitro*.

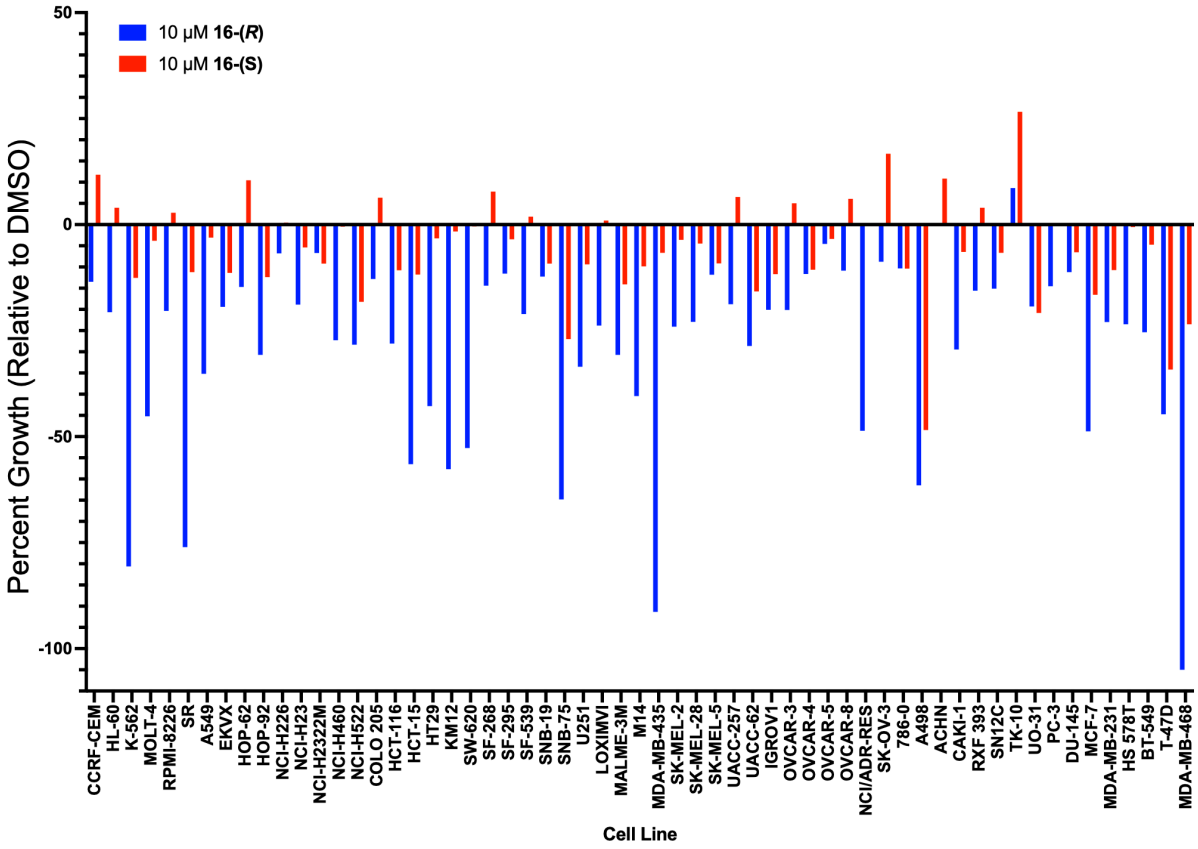

Figure 3.3. The Pin1 inhibitor 16-(*R*) but not control compound 16-(*S*) potently inhibits growth of a broad range of cancer cell lines. Pin1 inhibitor **16-(*R*)** and control molecule **16-(*S*)** were submitted to the NCI-60 growth inhibition cell line panel to determine Pin1-dependent cell lines. Each compound at 10 μM was used to inhibit the growth of each cell line in a 72-hour 2D growth inhibition experiment. Excitingly, many cell lines were determined to be partially inhibited by **16-(*R*)** and not **16-(*S*)**. Strikingly, K562, SR, HCT-15, KM12, SW-620, SNB-75, MDA-MB-435, and MDA-MB-468 cells were selectively inhibited >50% at 10 μM **16-(*R*)**. Interestingly, these represent diverse molecular oncologies; however Pin1's role in diverse biologies has been well documented in the literature (3).

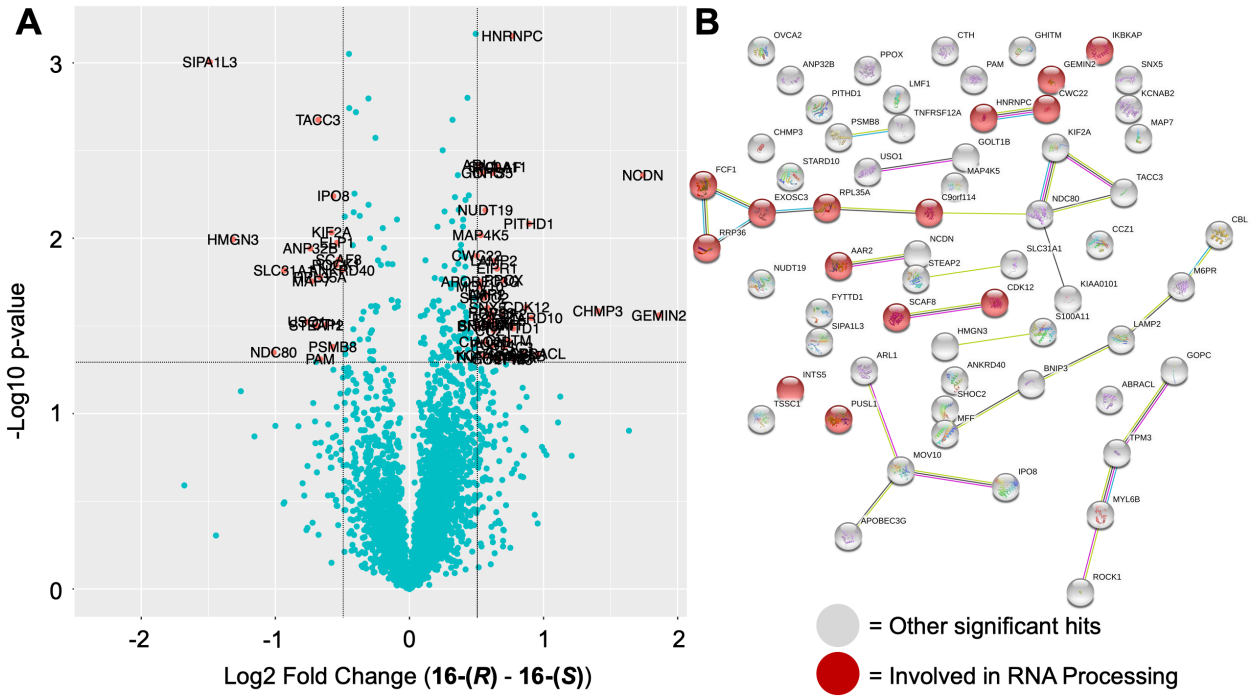

Figure 3.4. Pin1 inhibition rapidly down-regulates of RNA processing proteins. A) Results of a label-free quantitation proteomics experiment was done comparing cells treated with **16-(*R*)** with cells treated with **16-(*S*)**. Cells were treated for 24 hours with 250 nM of either compound. In this experiment, mild effects on the proteome were seen broadly. Excitingly, however, some protein abundances were perturbed significantly. Dashed lines indicate threshold for red-coloring and labeling proteins which had ≥1.5-fold change and p-value <0.05 in abundance between the two molecules. B) String-db plot of hit proteins thresholded as in A shows known interactions between the identified hits. Following gene ontology analysis, an enrichment of RNA processing proteins was identified. The corresponding spheres of RNA processing proteins are colored red.

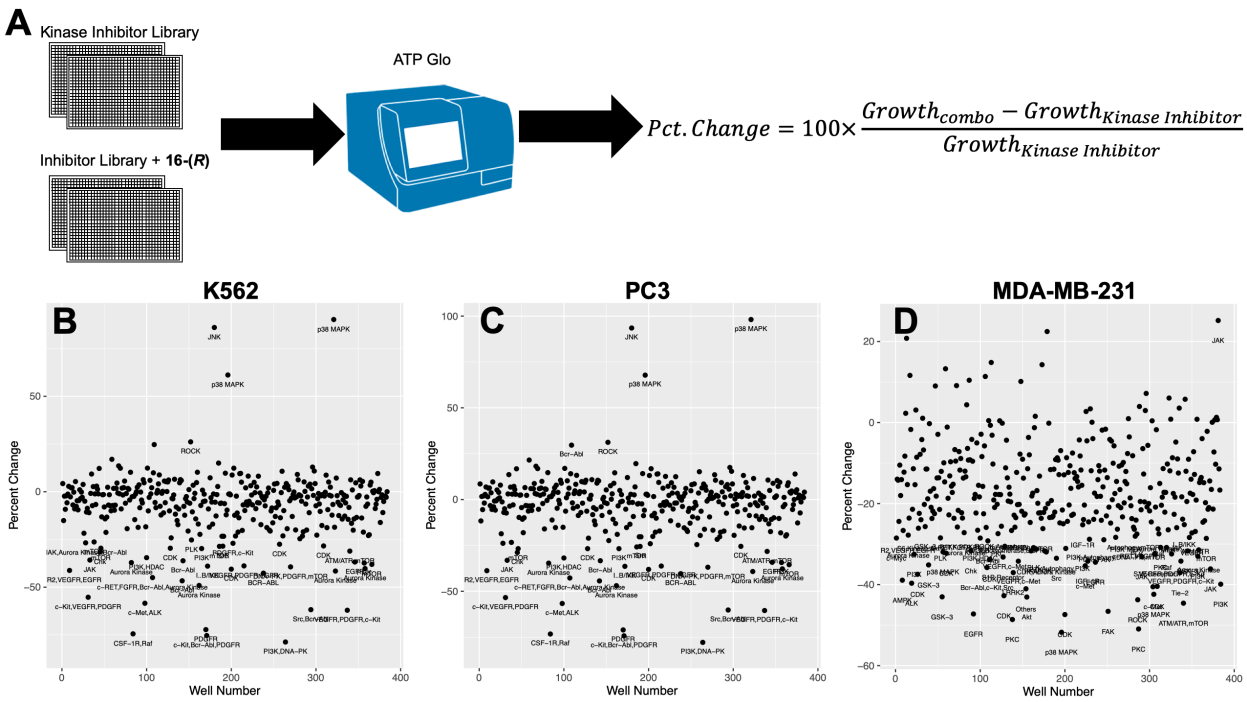

Figure 3.5. Pin1 inhibition potentiates many kinase inhibitors and enriched for PI3K/AKT/mTOR pathway cooperativity. A) Schematic of the screening method. Selleckchem 380-kinase inhibitor library was stamped onto 4 plates to yield a final concentration of 1 μM for each kinase inhibitor. These plates were then split into two replicates each of a DMSO or 250 nM **16-(*R*)** combination plates. Following 72-hour 2D growth, Cell Titer Glo reagent was added to the plates to assess percent growth as compared to DMSO controls. Importantly, 250 nM **16-(*R*)** imparts no growth defect on any of the cell lines tested in this format so all potentiation of the kinase inhibitor is non-additive. B) results of the K562 chronic myelogenous leukemia (CML) cell line screen show enrichment for RTK/PI3K/AKT/mTOR pathway inhibitors. This is consistent with the driver mutation of BCR-Abl fusion. Importantly, BCR-Abl inhibitors were also well-represented in the most potentiated kinase inhibitors. C) PC3 neuroendocrine prostate cancer cells rely on a similar pathway for growth as they harbor a PTEN loss leading to aberrantly active PI3K/AKT/mTOR signaling; consequently, the hits were strikingly similar between the K562 and PC3 screens. D) MDA-MB-231 triple-negative breast cancer cells have distinct driver mutations (i.e. KRAS, BRAF, and TP53 mutations) and interestingly had distinct hits in the potentiation screen. This cell line, interestingly enriched more proline-directed kinases in the list of most potentiated kinases, inspiring further exploration into the mechanisms of Pin1 potentiation of proline-directed kinases.

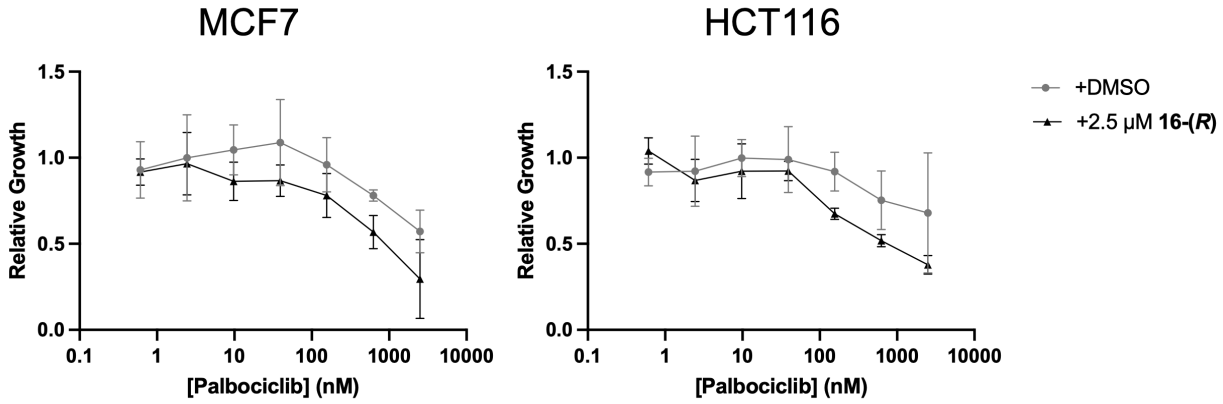

Figure 3.6. Pin1 inhibition cooperates with CDK4/6 inhibition in palbociclib-sensitive and -resistant cell lines. Pin1 inhibition potentiates the activity of the clinical CDK4/6 inhibitor palbociclib in the context of palbociclib-sensitive MCF7 (Her2-/ER+ breast cancer) and palbociclib-resistant HCT116 (colorectal cancer line with genomic instability and cyclin E1 overexpression). In both cases, there were doses at which Pin1 inhibition significantly potentiated the activity of palbociclib. Interestingly, In this assay, 2.5 μM **16-(*R*)** treatment alone had no growth defect.

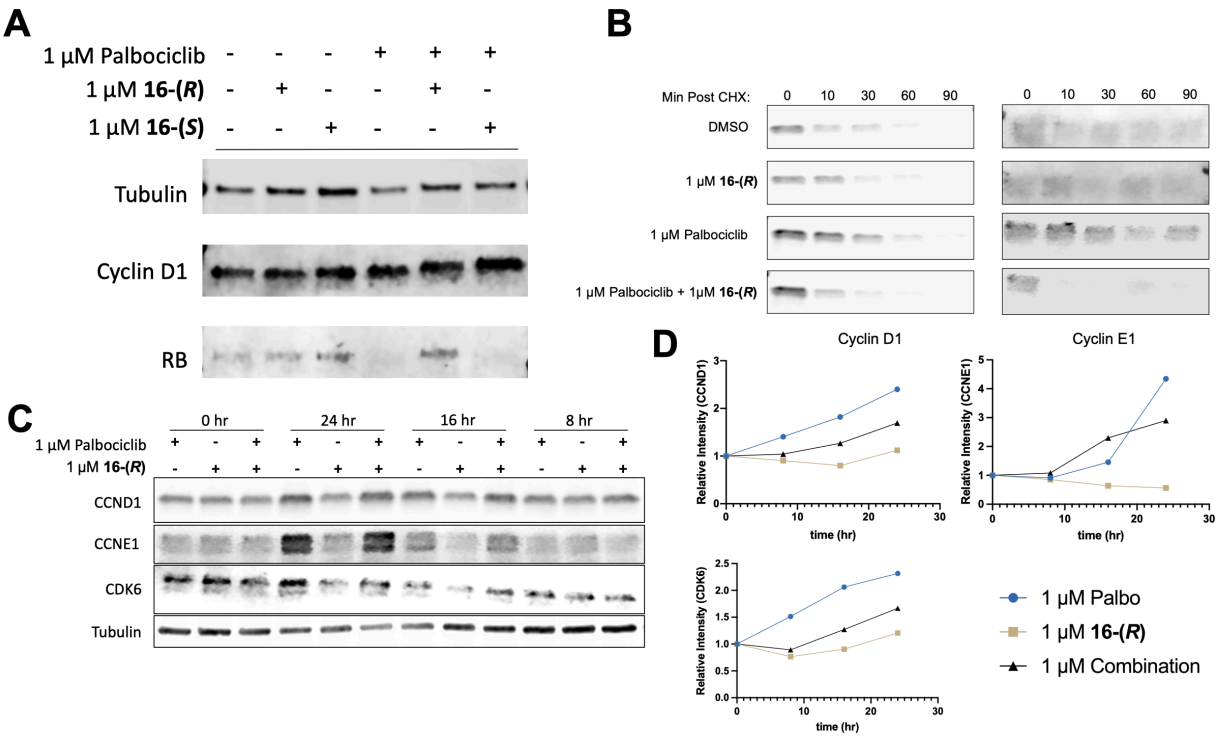

Figure 3.7. Pin1 inhibition destabilizes cyclin D1, E1 in and rescues palbociclib-induced Rb suppression in palbociclib-sensitive MCF7 cells. A) MCF7 cells were treated with single or combination inhibitor(s) for 24 hours While inhibition of Pin1 has no effect on cyclin D1 levels at steady state on this timescale, RB1 suppression in response to CDK4/6 inhibition was inhibited by **16-(*R*)** but not **16-(*S*)** co-treatment with palbociclib. B) MCF7 cells were treated for 18 hours with DMSO, 1 µM **16-(*R*)**, palbociclib, or combination followed by a time-course cycloheximide chase over 90 minutes. Interestingly, **16-(*R*)** treatment was more effective at destabilizing cyclins in combination with palbociclib treatment. C) 24-hour time-course observation of cyclin D1, E1, and CDK6 induction were evaluated with palbociclib, **16-(*R*)**, or combination treatment was conducted in MCF7 cells. Combination treatment had slower kinetics of induction of cyclin D1, cyclin E1, and CDK6 in response to palbociclib treatment.

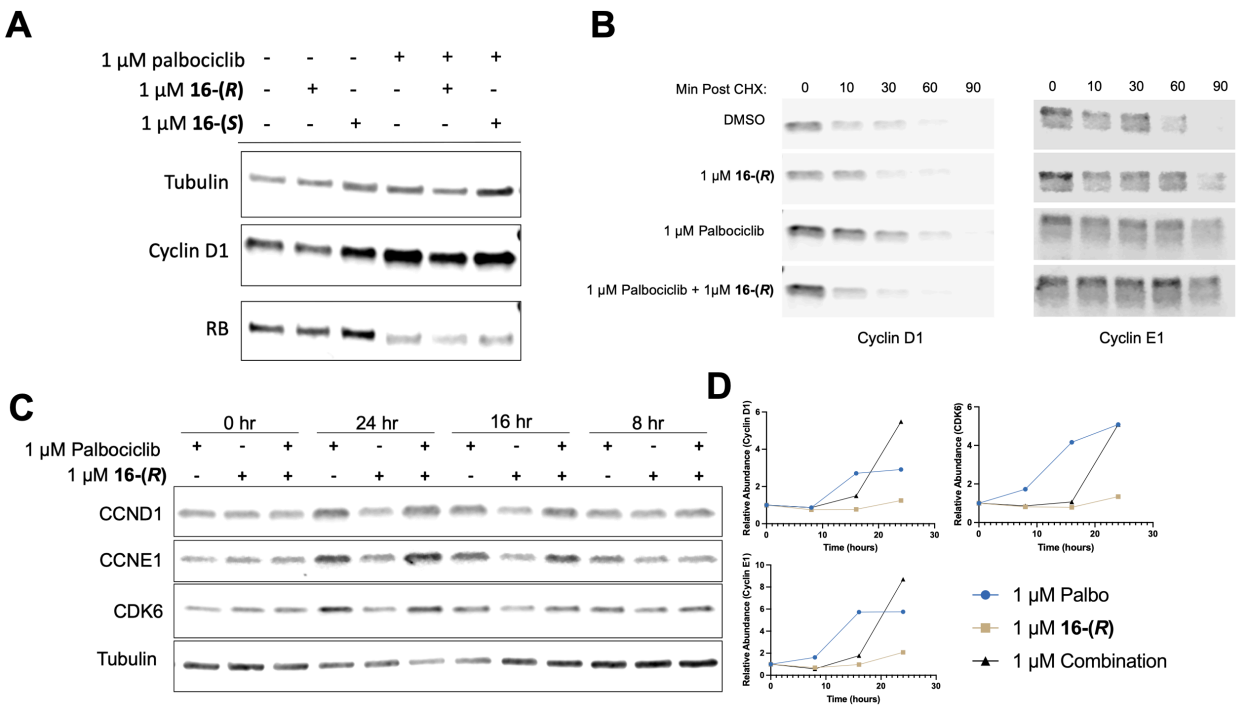

Figure 3.8. Pin1 inhibition reduces levels of cyclin D1 and cyclin E1 in palbociclib-resistant HCT116 cells. A) HCT116 cells were treated with single or combination inhibitor(s) for 24 hours. Distinct from the analogous MCF7 experiment (Figure 3.7) inhibition of Pin1 has decreased the concentration of cyclin D1 levels at steady state on this timescale, and RB1 suppression in response to CDK4/6 inhibition was no longer inhibited by **16-(*R*)** co-treatment with palbociclib. B) HCT116 cells were treated for 18 hours with DMSO, 1 µM **16-(*R*)**, palbociclib, or combination followed by a time-course cycloheximide chase over 90 minutes. Interestingly, **16-(*R*)** treatment and co-treatment were ineffective at destabilizing cyclins – again, distinct from what was seen in MCF7 cells. Indeed, it appears that cyclin E1 is stabilized by **16-(*R*)** treatment in both contexts. C) 24-hour time-course observation of cyclin D1, E1, and CDK6 induction were evaluated with palbociclib, **16-(*R*)**, or combination treatment was conducted in HCT116 cells. Combination treatment had slower kinetics of induction of cyclin D1, cyclin E1, and CDK6 in response to palbociclib treatment – consistent with what was seen in MCF7 cells.

Publishing Agreement

It is the policy of the University to encourage open access and broad distribution of all theses, dissertations, and manuscripts. The Graduate Division will facilitate the distribution of UCSF theses, dissertations, and manuscripts to the UCSF Library for open access and distribution. UCSF will make such theses, dissertations, and manuscripts accessible to the public and will take reasonable steps to preserve these works in perpetuity.

I hereby grant the non-exclusive, perpetual right to The Regents of the University of California to reproduce, publicly display, distribute, preserve, and publish copies of my thesis, dissertation, or manuscript in any form or media, now existing or later derived, including access online for teaching, research, and public service purposes.

Daniel M. Schwarz
Author Signature

6/9/2021
Date